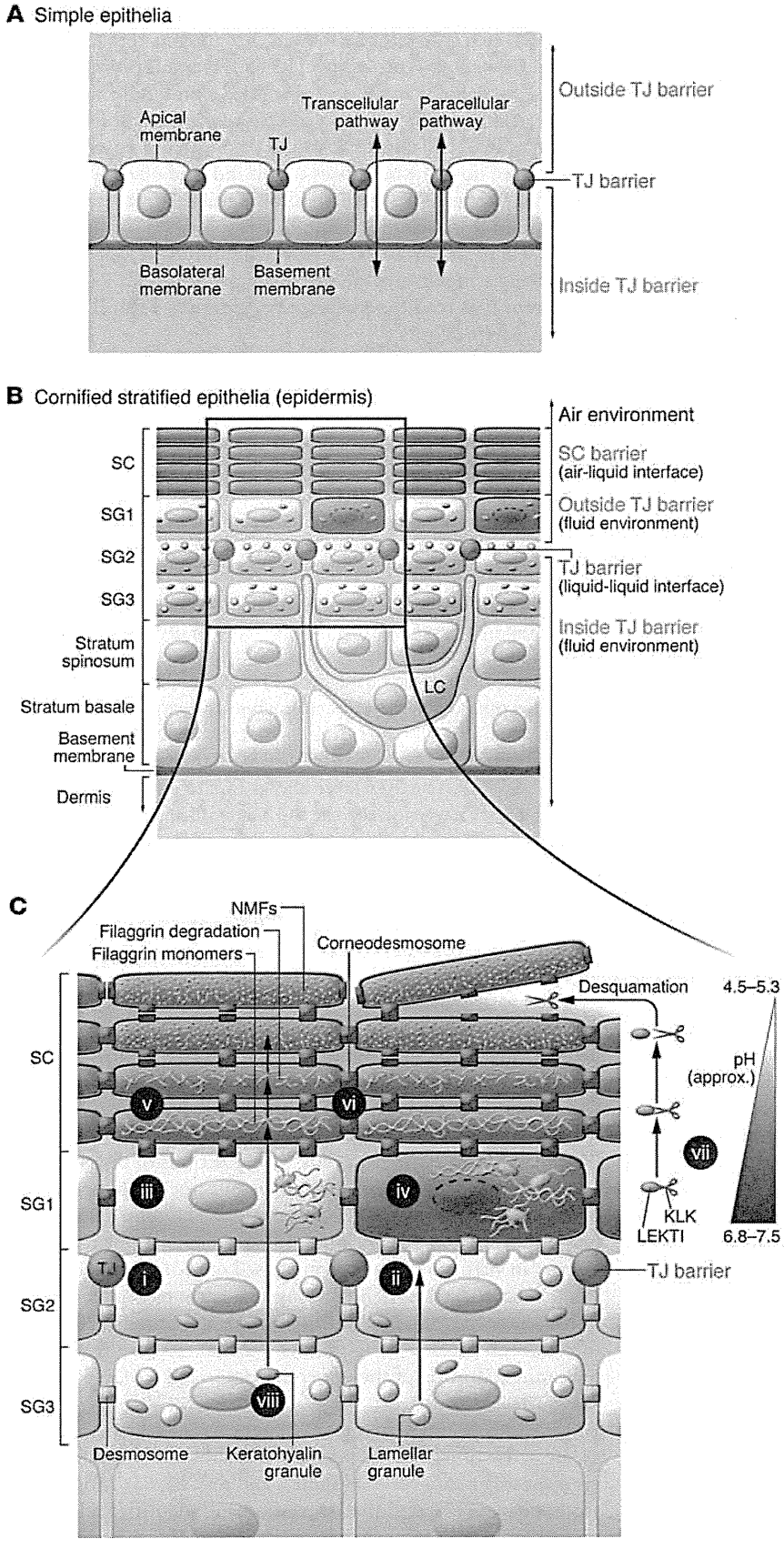

Figure 1
Schematic representation of the barriers in simple epithelia and stratified epidermis. (**A**) In simple epithelia, TJs seal the apical end of the lateral cell membrane. The extracellular fluid is compartmentalized into two parts by TJs. (**B**) In the mammalian epidermis, the SC serves as an air-liquid interface barrier and protects the living layers from desiccation. TJs also seal the paracellular spaces between SG2 cells. TJs act as a liquid-liquid interface barrier in both simple and cornified stratified epithelia. LCs position their dendrites upward, ready to survey antigens upon sensing perturbation. (**C**) Terminal differentiation in relation to TJs. When SG3 cells differentiate into SG2 cells, they form TJs (i) and begin to secrete lamellar granules from their apical membranes (ii). SG1 cells appear to lose their TJs (iii) and then undergo final cornification (iv). Mature corneocytes are encapsulated in the cornified envelope (dark brown; v), and their intercellular spaces are filled with lipid lamellae (brown). Corneodesmosomes (green squares; vi) mediate intercorneocyte adhesion. KLKs secreted into the extracellular space are strictly limited to the extra-TJ environment. As the pH becomes acidic in the upper layers of the SC, KLKs are released from LEKTI and proteolyze corneodesmosomes, initiating desquamation (vii). Profilaggrin is a component of keratohyalin granules in the SG, is degraded into filaggrin monomers, possibly in SG1 cells, and is further degraded into NMFs in the upper SC (viii).

the cell membrane (13, 22). From the apical membrane of SG2 cells, which correlate with the secretory granulocytes observed by electron microscopy (28), the contents of lamellar granules (e.g., lipids, extracellular structural proteins, hydrolytic enzymes, and various antibacterial peptides such as cathelicidin and β-defensin 2; refs. 29–31) begin to be secreted into, and are kept within, the extra-TJ compartment, where they form the intercellular structures of the SC (32). After SG2 cells differentiate into SG1 cells, they appear to lose their TJs and initiate the final cornification steps of terminal differentiation, which occur outside the TJ barrier within a distinct fluid compartment that is probably required for terminal differentiation. Based on the results of electron microscopic studies and immunofluorescence studies, the observed "transient cells" (33) are likely equivalent to SG1 cells (13, 22) undergoing cornification.

During cornification, SG1 cells are enucleated, lose intracellular organelles and cell membranes, and are encapsulated in a heavily cross-linked proteinous structure called the "cornified envelope" (34). Within the extra-TJ compartment, the adhesion complexes between SG1 cells, desmosomes, are modified to corneodesmosomes through the incorporation of corneodesmosin (29, 35). Paracellular spaces outside of the TJ start to be filled with a mixture of relatively nonpolar lipids enriched in ceramides, cholesterol, free fatty acids, and cholesterol esters, which are secreted from the apical ends of SG2 cells. These lipids form intercellular lipid lamellae, or the "mortar" of the SC. SG1 cells transform into the lowermost corneocytes, which are the "bricks" surrounded by the mortar. Multiple layers of this structure form the SC, outermost bricks of which are desquamated in a well-controlled process (described below).

Langerhans cells as an immune barrier. DCs are leukocyte subsets that specialize in antigen presentation and are distributed throughout the body to protect the body from microbial or antigenic insult. Several subsets of DCs reside in skin, and the Langerhans cells (LCs) are unique DCs of the epidermis, distinct from several subsets of dermal DCs (36, 37). Although LCs were long believed to be the initiators of immune responses in skin, several studies utilizing transgenic mice that allow selective targeting of DCs failed to demonstrate their critical contribution in hapten-induced contact hypersensitivity models (36, 37). However, more recent studies have demonstrated that LCs are indeed capable of inducing antigen-specific Th2 responses in vivo (38, 39).

Penetration of the TJ barrier by DC dendrites and subsequent uptake of extra-TJ antigens have been reported in the lamina propria of the intestine and bronchial epithelium and may also occur in nasal and adenoid epithelia (40–46). The epidermis, because of its stratification and two sets of barriers, is quite different from simple epithelia with regard to antigen penetration and the capture of antigens by DCs. Under steady-state conditions, LCs are on standby with their dendrites aimed outward, positioned close to, but never crossing, the TJ barrier (Figure 1B). SC barrier perturbation (e.g., tape-stripping or acetone treatment) has been known to stimulate cytokine production in the epidermis and/or to activate LCs (47–50). Once activated, LCs extend their dendrites through TJ barriers and take up antigens from the extra-TJ environment (Figure 2, Supplemental Video 2, and ref. 13). During this process, the tightness of the epidermal TJs is maintained by the de novo formation of TJs between keratinocytes and LCs, suggesting that LCs are able to take up foreign antigens from outside TJ barriers without penetrating these barriers (13). In contrast, dermal DCs presumably take up antigens that have penetrated both epidermal barriers. Ouchi et al. recently showed that antigen uptake through TJs by LCs leads to a protective Th2 (IgG1) humoral response in a mouse model of staphylococcal scalded skin syndrome (51). At present, it appears that LCs only induce a Th2 response in the presence of an intact TJ barrier. It would be of interest to explore the deviation of immune responses that is induced upon the disruption of TJ barriers, which might allow dermal DCs to have access to antigens, thus leading to immune responses not restricted to Th2. It will be important to assess such immune responses utilizing protein antigens that do not easily pass through TJs, instead of haptens that readily penetrate the epidermis, regardless of the barriers, to the dermis.

Dynamic cooperation and interaction of the three musketeers. As described above, the SC, TJs, and LCs together constitute a skin surface surveillance and barrier system. The SC directly faces the external environment, protecting the inner viable layers from desiccation. The SC is not a sterile surface but controls skin flora of microorganisms via antimicrobial peptides and low pH (52). The SG1 layer exists outside of the TJ barrier and its extracellular space is rich in various proteases, antimicrobial peptides, and, under certain circumstances, bacteria and bacteria-derived metabolites/antigens. TJs in the SG2 layer compartmentalize this layer from the viable layer, preventing the potentially pro-inflammatory molecules above it from perturbing immune signals (see below). LCs, positioned covertly under the TJs, are polarized to send their dendrites outside of the TJ barrier when activated by danger signals such as TSLP, TNF-α, and IL-1β, presumably secreted from keratinocytes that somehow detect SC damages (Figure 2 and refs. 47, 53–56). The SG1 layer allows LCs to sample for foreign materials that have violated the SC barrier (13). Thus these three musketeers work all for one, and one for all, to provide a highly organized skin barrier.

Major players in SC barrier dysfunction

Filaggrin mutations as predisposing factors for atopic diseases. Filaggrin is expressed in SG layers as a >400-kDa precursor protein, profilaggrin. Profilaggrin is the major component of the keratohyalin granules in SG cells. It is comprised of highly homologous tandem repeats of the filaggrin monomer (10–12 in humans and 16 in C57BL/6 mice), flanked by two imperfect repeats and N- and C-terminal domains. Profilaggrin is proteolyzed into filaggrin monomers and N- and C-terminal peptides at the boundary of the SC and SG, possibly in SG1 cells. The functions of the N- and C-terminal peptides are as yet unknown, but nuclear translocation of the former, which contains an S-100 Ca^{2+}-binding domain, has been reported (57). Filaggrin monomers display keratin-binding activity in vitro and have been proposed to promote the compaction of corneocytes by contributing to keratin pattern formation in the lower SC (58). Filaggrin monomers are further degraded into natural moisturizing factors (NMFs) that are thought to maintain hydration of the upper SC and to reduce the pH of the skin surfaces (59–61).

Mutations in the filaggrin (*FLG*) gene were identified initially as the cause of ichthyosis vulgaris and subsequently as a major predisposing factor for AD (Table 1 and refs. 62, 63). More recent studies have confirmed the association and identified additional mutations in the *FLG* gene that predispose to AD in European and Asian populations (64–67). *FLG* mutations have also been reported to be associated with atopic asthma, allergic rhinitis, nickel allergy,

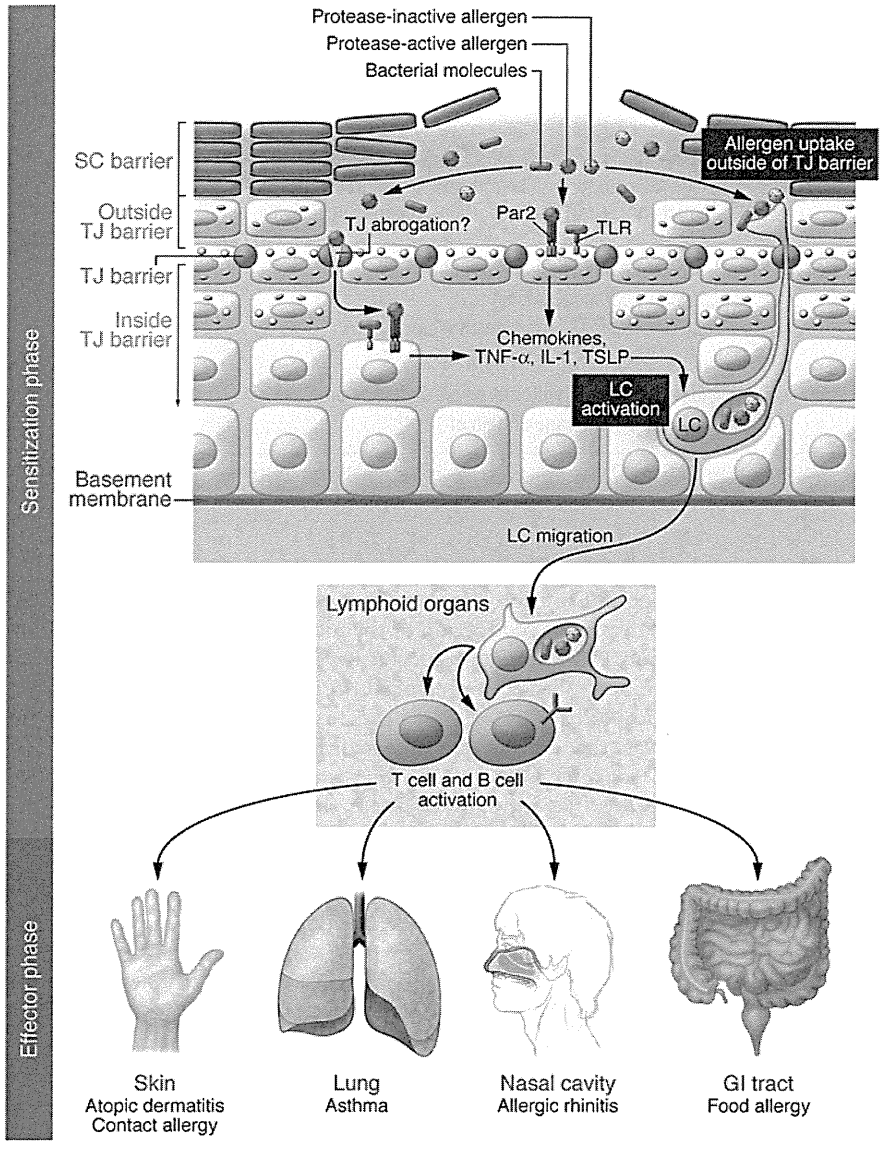

Figure 2
A model of barrier disruption and consequences of percutaneous sensitization. SC barrier damages induce danger signals in the epidermis. After SC barrier abrogation, protease-active allergens and uncontrolled intrinsic proteases, as well as bacterial molecules such as lipoteichoic acid of gram-positive bacteria, might agonize Par2 and TLRs on keratinocytes, respectively (7, 55, 112, 123). Keratinocytes then produce TNF-α, IL-1, and thymic stromal lymphopoietin (TSLP) (47, 55), in response to which LCs become activated (54, 56, 124). Alternatively, protease-active allergens might directly obscure the TJ barrier and then penetrate the epidermis (7), where they directly or indirectly activate LCs. Upon SC perturbation, dendrites of activated LCs penetrate the TJs to take up protease-active or -inactive antigens from the extra-TJ environment (13). Such percutaneous sensitization and chronic allergen challenge via different routes, such as the lungs, nasal cavities, and intestinal tract, are speculated to manifest as the atopic march.

and food allergy (68–73), suggesting that *FLG* mutation–associated SC barrier defects lead to increased numbers of episodes of percutaneous allergen exposure (Figure 2). Interestingly, *FLG* mutations are not associated with asthma without eczema (70, 71), and most of the identified asthma-associated genes are not associated with AD (74, 75), suggesting that atopic asthma is a distinguishable sub-entity. Because filaggrin is not expressed in the upper airways (76), systemic sensitization is likely attributable to percutaneous antigen exposure through filaggrin-deficient skin. In good agreement with this hypothesis, percutaneous sensitization induces allergic responses to allergens in mice challenged via the upper airway (77, 78). Further investigation is required to clarify the impact of filaggrin deficiency on the barrier function of SC and the molecular mechanisms of percutaneous sensitization in the pathophysiology of AD and atopic diseases.

Mouse models of filaggrin deficiency. Flaky tail (ft) mice were created in 1958 on the background of an existing recessive hair phenotype, matted (ma), and also exhibited dry, flaky skin with annular tail and paw constrictions during the neonatal period (79). Since then, they have been maintained in a mixed strain (ft/ma) (80). The ft mutation was found to be a 1-bp deletion in filaggrin repeat 6, which leads to premature termination, analogous to common human *FLG* mutations (81). ft/ma mice show paracellular barrier permeability in SC (82), increased trans-epidermal water loss (TEWL), and enhanced percutaneous allergen priming (83). They also spontaneously develop dermatitis under steady-state conditions (83) and have been used as a model of filaggrin deficiency and AD. However, ma locus-eliminated homozygous ft mice (identified by the absence of matted hair) only show mild diffuse hypertrophy of the SC and sporadic superficial dermal cellular infiltrates under steady-state conditions (81). Furthermore, while ft/ma mice show elevated TEWL (83), ft mice show no statistically significant difference in baseline TEWL (81). Thus, when ft/ma mice are used in studies of AD in the context of filaggrin deficiency, the results need to be interpreted carefully. It would be of interest to identify the gene responsible for the ma phenotype, and the gene's function, to understand the pathophysiological mechanisms behind the spontaneous development of dermatitis in ft/ma mice.

Table 1
Skin barrier–related genes associated with AD/AD-like dermatitis

Gene symbol	Gene name	Functions	Representative refs.[A]
Filaggrin system			
FLG	Filaggrin	Major constituent of keratohyalin granules; bundling keratin filament to form keratin pattern; degradation products are reported to have skin-moisturizing activity	62, 69
Desquamation			
SPINK5	Serine peptidase inhibitor, Kazal type 5	pH-dependent inhibition of KLK5 and KLK7	86
KLK7[B]	Kallikrein-related peptidase 7	Digestion of corneodesmosin	96
CDSN	Corneodesmosin	Structural protein of corneodesmosomes	97[C]
Others			
CSTA	Cystatin A	Cysteine protease inhibitor of house dust mite protease	125
CLDN1[D]	Claudin 1	Integral transmembrane protein of TJs	109

[A]For more detailed data on gene variants, see ref. 75. [B]The association with AD is still controversial (126). [C]Only reported as responsible for peeling skin syndrome type B. [D]No atopic disease has been reported to complicate in patients with NISCH, who totally lack claudin 1 protein (107, 108).

Hereditary SC barrier deficiency with complicating atopic disease. Desquamation is a well-orchestrated process controlled by a network of proteases, which themselves are regulated by protease inhibitors and skin pH. Among these, kallikrein-related (KLK-related) peptidases and their pH-dependent inhibition by lymphoepithelial Kazal type–related inhibitor (LEKTI; encoded by serine peptidase inhibitor, Kazal type 5 [*SPINK5*] gene) are the best characterized (Figure 1B and refs. 84, 85). Under normal conditions, the neutral pH in the lower SC enables LEKTI to inactivate KLK5 and KLK7, while the acidic conditions in the uppermost part of the SC inhibit LEKTI, thereby allowing KLK5 and KLK7 to function and thus promoting skin peeling. Genetic studies have demonstrated linkage between polymorphisms in *SPINK5* and AD, asthma, and elevated levels of serum IgE (86–88). Loss of function of *SPINK5* causes Netherton syndrome, a severe autosomal recessive ichthyosis characterized by chronic dermatitis, asthma, and allergic rhinitis (89). Ultrastructural analyses show a marked increase in corneodesmosome cleavage and SC detachment at the border between transient cells and SG cells in the skin of patients with Netherton syndrome (90–92). Studies of *SPINK5*-knockout mice confirmed that LEKTI deficiency results in elevated KLK5 activity in the layers of the SC and subsequent breakdown of corneodesmosin, followed by SC barrier loss (93–95). Polymorphisms in *SPINK5* and *KLK7* associated with AD may produce a similar, but milder, SC barrier defect (Table 1 and refs. 86, 96). Genetic loss of corneodesmosin causes peeling skin syndrome type B, in which the whole SC is easily detached from the underlying living layers, leading to chronic dermatitis, asthma, allergic rhinitis, elevated levels of serum IgE, and food allergy (Table 1 and ref. 97), suggesting that SC barrier dysfunction precedes the onset of atopic diseases.

Loss of the SC barrier, as occurs in Netherton syndrome and peeling skin syndrome type B, induces dermatitis, asthma, and allergic rhinitis, suggesting that perturbation of the desquamation processes could induce SC barrier defects and predispose to AD or similar conditions. Overexpression of elastase 2 and over degradation of profilaggrin were recently reported in the skin of patients with Netherton syndrome (98), and it is necessary to evaluate whether the filaggrin system malfunction plays a direct role on the barrier dysfunction in these two diseases. Interestingly, under LEKTI-deficient conditions (as in Netherton syndrome), spontaneous protease-activated receptor 2 (Par2) activation and subsequent production of thymic stromal lymphopoietin, IL-8, and TNF-α in keratinocytes have been reported to result from uncontrolled activation of KLK5, indicating that aberrant activation of barrier-associated proteases can modulate immunity in ways that exacerbate atopic manifestations (55).

Search for additional candidate genes in atopic diseases. As mentioned above, filaggrin mutations are, thus far, the major predisposing factor for classic atopy. However, such mutations are not found in a significant number of patients, indicating that other genetic factors that influence skin barrier function may also be important. Candidate molecules include enzymes that function in the degradation of profilaggrin (61). Retroviral-like aspartic protease (SASPase) is a skin-specific protease that directly cleaves a linker peptide in profilaggrin. Hairless mice deficient in SASPase exhibit dry skin and aberrantly processed profilaggrin accumulation in the lower SC (99). Caspase-14 is a skin-specific enzyme that may be involved in the early degradation of filaggrin monomers to NMFs, and caspase-14–knockout mice display a dry skin phenotype (100, 101). Bleomycin hydrolase has been reported to be involved in a later stage of the degradation processes (102, 103). Bleomycin hydrolase–knockout mice display generalized scaling and mild ichthyosis in their neonatal period, while adults appear normal but develop low-humidity-induced dermatitis in their tails (104). Further epidemiological studies are warranted to determine whether mutations in these proteases are predisposing factors for human AD.

TJ barriers may also be involved in proper SC formation. Claudin 1 is one of the major integral transmembrane components of epidermal TJs, and in claudin 1–knockout mice, epidermal TJs lose tightness and the SC displays compact hyperkeratosis, suggesting that loss of tightness of the TJ barrier may also affect terminal differentiation in the epidermis (22). Ectopic overexpression of periderm-specific claudin, claudin 6, in the SG induces a phenotype that is identical to claudin 1–knockout mice (105, 106), suggesting that differential expression or the balance of claudin molecules might regulate the tightness of TJ barriers. Patients with neonatal ichthyosis and sclerosing cholangitis (NISCH) have homozygous nonsense mutations in the claudin 1 gene and display ichthyosis, further suggesting the

involvement of the TJ barrier in proper SC formation (107, 108). Interestingly, a polymorphism in the claudin 1 gene was recently reported as a possible candidate mutation in AD (Table 1 and ref. 109). Further large-scale epidemiological studies and careful investigation of the crosstalk between the TJ and SC barriers are necessary to assess the contribution of TJs to the pathogenesis of AD.

Percutaneous sensitization through insufficient SC barrier

LC activation induced by SC barrier perturbation. In contrast to the above-described congenital diseases that affect the SC, the entire epidermis is lost in junctional or dystrophic epidermolysis bullosa (EB) (110). Interestingly, patients with EB do not usually develop atopic diseases, and genes responsible for EB, such as those that encode laminin 332, and the type VII and XVII collagens, were not identified in genome-wide linkage studies of AD or asthma. Thus, living layer structures of the epidermis and cellular immune components, such as LCs, may be required for the development of atopic diseases. In this context, it is important to understand how foreign antigens or allergens are taken up within the epidermis and presented to the immune system (12, 51).

To induce epicutaneous sensitization to protein antigens in mice, the tough SC barrier needs to be mechanically impaired by tape-stripping, acetone treatment, or patch dressing (78). Interestingly, tape-stripping mouse ear skin activates LCs and induces penetration of the TJ barrier by LC dendrites, suggesting that causing physical stress to the SC induces danger signals in epidermis that directly or indirectly activate LCs (Figure 2 and refs. 13, 47, 50, 53–56). Thus, perturbation of the SC barrier not only allows allergen penetration throughout this barrier, but also triggers LC activation and facilitates subsequent uptake of antigens by LCs across the epidermal TJ barrier. After antigen acquisition, LCs presumably migrate to draining lymph nodes and activate antigen-specific T cells. Although danger signals similar to those observed in simple epithelium models, such as the lungs, may also occur in skin, as shown in Figure 2 (7, 53, 111–114), it is not yet clear how LCs sense danger signals caused by SC damage, and the specific signals that are delivered across the TJ barrier remain to be investigated.

The chicken or the egg in atopic diseases. Skin barrier defects and immune disorders present a chicken and egg dilemma in AD. Allergens that have penetrated defective skin barriers induce inflammation, while inflammation itself can alter skin barrier integrity. Th2 and Th17 cytokines have been reported to downregulate filaggrin expression or proper processing of profilaggrin (115–119). Not only genetic skin barrier defects, but also genetic immune disorders such as Wiskott-Aldrich syndrome, show atopic manifestations (120), indicating that AD emerges in the context of both epidermal barrier- and immunity-associated genetic dysfunction. Indeed, many immunity-associated genes, e.g., Th2 and Th17 cytokines, innate immune receptors, and various chemokines, have been identified through whole-genome linkage studies of susceptibility genes for atopic diseases (75), some of which have been reported to show a multiplicative effect with *FLG* mutations on AD (121). It seems reasonable to suggest that immunity-associated genetic factors, as well as environmental factors, may act additively (or synergistically) to produce SC barrier defects and to promote percutaneous sensitization during the onset of AD.

Conquering the epidermal barrier is a double victory

Epidermal barriers face harsh challenges in modern life. Features of current lifestyles, such as frequent bathing and regular use of soap, and living within concrete jungles with air conditioning that dehumidifies the air, may accelerate SC barrier impairment (11). Constant heating, decreased ventilation, and floors covered with carpets are likely to increase house dust mite numbers and allergen levels in living environments. These environments, which expose the skin to both mechanical and allergic cues, may induce not only SC barrier damage but also danger signals that activate LCs, and could be a part of the reason why the prevalence of atopic diseases is increasing in industrialized countries (2). *FLG* mutations are associated with not only AD, but also atopic asthma, allergic rhinitis, and food allergy, emphasizing the importance of percutaneous sensitization as an initial trigger of atopic cascades, which lead to the atopic march (Figure 2). A simple and straightforward approach to preventing or controlling atopic cascades is to maintain intact epidermal barriers after birth or after improvement of acute inflammation (122). Clarification of the exact molecular functions of the epidermal barrier, with the SC as an air-liquid interface barrier, TJs as a liquid-liquid interface barrier, and LCs as an immunological barrier, will lead to a more sophisticated understanding as well as practical solutions for conquering atopic diseases.

Acknowledgments

This work was supported by Grants-in-Aid for Scientific Research and the "Promotion of Environmental Improvement for Independence of Young Researchers" program funding from the Ministry of Education, Culture, Sports, Science and Technology of Japan, and by Health Labour Sciences Research Grants for Research on Allergic Diseases and Immunology from the Ministry of Health, Labour, and Welfare of Japan.

Address correspondence to: Masayuki Amagai, Department of Dermatology, Keio University School of Medicine, Shinanomachi 35, Shinjuku, Tokyo 160-8582, Japan. Phone: 81.3.53633822; Fax: 81.3.33516880; E-mail: amagai@a7.keio.jp.

1. Spergel JM. From atopic dermatitis to asthma: the atopic march. *Ann Allergy Asthma Immunol.* 2010;105(2):99–106.
2. Bieber T. Atopic dermatitis. *N Engl J Med.* 2008; 358(14):1483–1494.
3. Furuse M, Tsukita S. Claudins in occluding junctions of humans and flies. *Trends Cell Biol.* 2006; 16(4):181–188.
4. Cookson W. The immunogenetics of asthma and eczema: a new focus on the epithelium. *Nat Rev Immunol.* 2004;4(12):978–988.
5. Hackett T-L, Knight DA. The role of epithelial injury and repair in the origins of asthma. *Curr Opin Allergy Clin Immunol.* 2007;7(1):63–68.
6. Xavier RJ, Podolsky DK. Unravelling the pathogenesis of inflammatory bowel disease. *Nature.* 2007;448(7152):427–434.
7. Hammad H, Lambrecht BN. Dendritic cells and epithelial cells: linking innate and adaptive immunity in asthma. *Nat Rev Immunol.* 2008;8(3):193–204.
8. McGrath JA, Uitto J. The filaggrin story: novel insights into skin-barrier function and disease. *Trends Mol Med.* 2008;14(1):20–27.
9. Schulzke JD, et al. Epithelial tight junctions in intestinal inflammation. *Ann N Y Acad Sci.* 2009;1165:294–300.
10. Turner JR. Intestinal mucosal barrier function in health and disease. *Nat Rev Immunol.* 2009;9(11):799–809.
11. Cork MJ, et al. Epidermal barrier dysfunction in atopic dermatitis. *J Invest Dermatol.* 2009; 129(8):1892–1908.
12. Beck LA, Leung DY. Allergen sensitization through the skin induces systemic allergic responses. *J Allergy Clin Immunol.* 2000;106(5 suppl):S258–S263.
13. Kubo A, Nagao K, Yokouchi M, Sasaki H, Amagai

M. External antigen uptake by Langerhans cells with reorganization of epidermal tight junction barriers. *J Exp Med.* 2009;206(13):2937–2946.
14. Aberg KM, et al. Co-regulation and interdependence of the mammalian epidermal permeability and antimicrobial barriers. *J Invest Dermatol.* 2008;128(4):917–925.
15. Tsukita S, Furuse M, Itoh M. Multifunctional strands in tight junctions. *Nat Rev Mol Cell Biol.* 2001;2(4):285–293.
16. Tsukita S, Yamazaki Y, Katsuno T, Tamura A. Tight junction-based epithelial microenvironment and cell proliferation. *Oncogene.* 2008; 27(55):6930–6938.
17. Anderson JM, Van Itallie CM. Physiology and function of the tight junction. *Cold Spring Harb Perspect Biol.* 2009;1(2):a002584.
18. Farquhar MG, Palade GE. Cell junctions in amphibian skin. *J Cell Biol.* 1965;26(1):263–291.
19. Mittal AK, Whitear M. Keratinization of fish skin with special reference to the catfish Bagarius bagarius. *Cell Tissue Res.* 1979;202(2):213–230.
20. Hashimoto K. Intercellular spaces of the human epidermis as demonstrated with lanthanum. *J Invest Dermatol.* 1971;57(1):17–31.
21. Landmann L, Stolinski C, Martin B. The permeability barrier in the epidermis of the grass snake during the resting stage of the sloughing cycle. *Cell Tissue Res.* 1981;215(2):369–382.
22. Furuse M, et al. Claudin-based tight junctions are crucial for the mammalian epidermal barrier: a lesson from claudin-1-deficient mice. *J Cell Biol.* 2002;156(6):1099–1111.
23. Brandner JM, et al. Organization and formation of the tight junction system in human epidermis and cultured keratinocytes. *Eur J Cell Biol.* 2002;81(5):253–263.
24. Tsukita S, Furuse M. Claudin-based barrier in simple and stratified cellular sheets. *Curr Opin Cell Biol.* 2002;14(5):531–536.
25. Mackenzie IC. Relationship between mitosis and the ordered structure of the stratum corneum in mouse epidermis. *Nature.* 1970;226(5246):653–655.
26. Christophers E. Cellular architecture of the stratum corneum. *J Invest Dermatol.* 1971;56(3):165–169.
27. Mackenzie IC. Ordered structure of the epidermis. *J Invest Dermatol.* 1975;65(1):45–51.
28. Elias PM, et al. The secretory granular cell: the outermost granular cell as a specialized secretory cell. *J Invest Dermatol Symp Proc.* 1998;3(2):87–100.
29. Ishida-Yamamoto A, et al. Epidermal lamellar granules transport different cargoes as distinct aggregates. *J Invest Dermatol.* 2004;122(5):1137–1144.
30. Braff MH, Di Nardo A, Gallo RL. Keratinocytes store the antimicrobial peptide cathelicidin in lamellar bodies. *J Invest Dermatol.* 2005; 124(2):394–400.
31. Oren A, Ganz T, Liu L, Meerloo T. In human epidermis, beta-defensin 2 is packaged in lamellar bodies. *Exp Mol Pathol.* 2003;74(2):180–182.
32. Kuroda S, et al. Perturbation of lamellar granule secretion by sodium caprate implicates epidermal tight junctions in lamellar granule function. *J Dermatol Sci.* 2010;59(2):107–114.
33. Montagna W, Parakkal P. *The Structure And Function Of Skin.* Orlando, Florida, USA: Academic Press; 1974.
34. Candi E, Schmidt R, Melino G. The cornified envelope: a model of cell death in the skin. *Nat Rev Mol Cell Biol.* 2005;6(4):328–340.
35. Simon M, et al. Refined characterization of corneodesmosin proteolysis during terminal differentiation of human epidermis and its relationship to desquamation. *J Biol Chem.* 2001; 276(23):20292–20299.
36. Kaplan DH. In vivo function of Langerhans cells and dermal dendritic cells. *Trends Immunol.* 2010;31(12):446–451.
37. Merad M, Ginhoux F, Collin M. Origin, homeostasis and function of Langerhans cells and other langerin-expressing dendritic cells. *Nat Rev Immunol.* 2008;8(12):935–947.
38. Nagao K, et al. Murine epidermal Langerhans cells and langerin-expressing dermal dendritic cells are unrelated and exhibit distinct functions. *Proc Natl Acad Sci U S A.* 2009;106(9):3312–3317.
39. Elentner A, et al. Langerhans cells are critical in the development of atopic dermatitis-like inflammation and symptoms in mice. *J Cell Mol Med.* 2009;13(8B):2658–2672.
40. Rescigno M, et al. Dendritic cells express tight junction proteins and penetrate gut epithelial monolayers to sample bacteria. *Nat Immunol.* 2001;2(4):361–367.
41. Ichiyasu H, McCormack JM, McCarthy KM, Dombkowski D, Preffer FI, Schneeberger EE. Matrix metalloproteinase-9-deficient dendritic cells have impaired migration through tracheal epithelial tight junctions. *Am J Respir Cell Mol Biol.* 2004;30(6):761–770.
42. Niess JH, et al. CX3CR1-mediated dendritic cell access to the intestinal lumen and bacterial clearance. *Science.* 2005;307(5707):254–258.
43. Takano K, et al. HLA-DR- and CD11c-positive dendritic cells penetrate beyond well-developed epithelial tight junctions in human nasal mucosa of allergic rhinitis. *J Histochem Cytochem.* 2005;53(5):611–619.
44. Chieppa M, Rescigno M, Huang AYC, Germain RN. Dynamic imaging of dendritic cell extension into the small bowel lumen in response to epithelial cell TLR engagement. *J Exp Med.* 2006;203(13):2841–2852.
45. Blank F, Rothen-Rutishauser B, Gehr P. Dendritic cells and macrophages form a transepithelial network against foreign particulate antigens. *Am J Respir Cell Mol Biol.* 2007;36(6):669–677.
46. Ogasawara N, et al. Epithelial barrier and antigen uptake in lymphoepithelium of human adenoids. *Acta Otolaryngol.* 2011;131(2):116–123.
47. Wood LC, Jackson SM, Elias PM, Grunfeld C, Feingold KR. Cutaneous barrier perturbation stimulates cytokine production in the epidermis of mice. *J Clin Invest.* 1992;90(2):482–487.
48. Streilein JW, Lonsberry LW, Bergstresser PR. Depletion of epidermal langerhans cells and Ia immunogenicity from tape-stripped mouse skin. *J Exp Med.* 1982;155(3):863–871.
49. Lessard RJ, Wolff K, Winkelmann RK. The disappearance and regeneration of Langerhans cells following epidermal injury. *J Invest Dermatol.* 1968;50(2):171–179.
50. Nishijima T, Tokura Y, Imokawa G, Seo N, Furukawa F, Takigawa M. Altered permeability and disordered cutaneous immunoregulatory function in mice with acute barrier disruption. *J Invest Dermatol.* 1997;109(2):175–182.
51. Ouchi T, et al. Langerhans cell antigen capture through tight junctions confers preemptive immunity in experimental staphylococcal scalded skin syndrome. *J Exp Med.* 2011;208(13):2607–2613.
52. Schröder JM, Harder J. Antimicrobial skin peptides and proteins. *Cell Mol Life Sci.* 2006;63(4):469–486.
53. Dai X, et al. Mite allergen is a danger signal for the skin via activation of inflammasome in keratinocytes. *J Allergy Clin Immunol.* 2011;127(3):806–814.
54. Nishibu A, Ward BR, Boes M, Takashima A. Roles for IL-1 and TNFalpha in dynamic behavioral responses of Langerhans cells to topical hapten application. *J Dermatol Sci.* 2007;45(1):23–30.
55. Briot A, et al. Kallikrein 5 induces atopic dermatitis-like lesions through PAR2-mediated thymic stromal lymphopoietin expression in Netherton syndrome. *J Exp Med.* 2009;206(5):1135–1147.
56. Ebner S, et al. Thymic stromal lymphopoietin converts human epidermal Langerhans cells into antigen-presenting cells that induce proallergic T cells. *J Allergy Clin Immunol.* 2007;119(4):982–990.
57. Pearton DJ, Dale BA, Presland RB. Functional analysis of the profilaggrin N-terminal peptide: identification of domains that regulate nuclear and cytoplasmic distribution. *J Invest Dermatol.* 2002;119(3):661–669.
58. Dale BA, Holbrook KA, Steinert PM. Assembly of stratum corneum basic protein and keratin filaments in macrofibrils. *Nature.* 1978;276(5689):729–731.
59. Scott IR, Harding CR. Filaggrin breakdown to water binding compounds during development of the rat stratum corneum is controlled by the water activity of the environment. *Dev Biol.* 1986;115(1):84–92.
60. Rawlings AV, Matts PJ. Stratum corneum moisturization at the molecular level: an update in relation to the dry skin cycle. *J Invest Dermatol.* 2005;124(6):1099–1110.
61. Sandilands A, Sutherland C, Irvine AD, McLean WHI. Filaggrin in the frontline: role in skin barrier function and disease. *J Cell Sci.* 2009; 122(9):1285–1294.
62. Smith FJD, et al. Loss-of-function mutations in the gene encoding filaggrin cause ichthyosis vulgaris. *Nat Genet.* 2006;38(3):337–342.
63. Palmer CN, et al. Common loss-of-function variants of the epidermal barrier protein filaggrin are a major predisposing factor for atopic dermatitis. *Nat Genet.* 2006;38(4):441–446.
64. Sandilands A, et al. Comprehensive analysis of the gene encoding filaggrin uncovers prevalent and rare mutations in ichthyosis vulgaris and atopic eczema. *Nat Genet.* 2007;39(5):650–654.
65. O'Regan GM, Sandilands A, McLean WHI, Irvine AD. Filaggrin in atopic dermatitis. *J Allergy Clin Immunol.* 2008;122(4):689–693.
66. Akiyama M. FLG mutations in ichthyosis vulgaris and atopic eczema: spectrum of mutations and population genetics. *Br J Dermatol.* 2010;162(3):472–477.
67. Poninska J, et al. Filaggrin gene defects are independent risk factors for atopic asthma in a Polish population: a study in ECAP cohort. *PLoS ONE.* 2011;6(2):e16933.
68. Basu K, et al. Filaggrin null mutations are associated with increased asthma exacerbations in children and young adults. *Allergy.* 2008;63(9):1211–1217.
69. Novak N, et al. Loss-of-function mutations in the filaggrin gene and allergic contact sensitization to nickel. *J Invest Dermatol.* 2008;128(6):1430–1435.
70. Rodríguez E, et al. Meta-analysis of filaggrin polymorphisms in eczema and asthma: robust risk factors in atopic disease. *J Allergy Clin Immunol.* 2009;123(6):1361–1370.
71. Schuttelaar MLA, et al. Filaggrin mutations in the onset of eczema, sensitization, asthma, hay fever and the interaction with cat exposure. *Allergy.* 2009;64(12):1758–1765.
72. Thyssen JP, et al. The association between null mutations in the filaggrin gene and contact sensitization to nickel and other chemicals in the general population. *Br J Dermatol.* 2010;162(6):1278–1285.
73. Brown SJ, et al. Loss-of-function variants in the filaggrin gene are a significant risk factor for peanut allergy. *J Allergy Clin Immunol.* 2011;127(3):661–667.
74. Vercelli D. Discovering susceptibility genes for asthma and allergy. *Nat Rev Immunol.* 2008;8(3):169–182.
75. Barnes KC. An update on the genetics of atopic dermatitis: scratching the surface in 2009. *J Allergy Clin Immunol.* 2010;125(1):16–29.
76. De Benedetto A, Qualia CM, Baroody FM, Beck LA. Filaggrin expression in oral, nasal, and esophageal mucosa. *J Invest Dermatol.* 2008;128(6):1594–1597.
77. Kodama M, et al. Strain-specific phenotypes of airway inflammation and bronchial hyperresponsiveness induced by epicutaneous allergen sensitization in BALB/c and C57BL/6 mice. *Int Arch Allergy Immunol.* 2010;152 suppl 1:67–74.
78. Spergel JM, Mizoguchi E, Brewer JP, Martin TR,

Bhan AK, Geha RS. Epicutaneous sensitization with protein antigen induces localized allergic dermatitis and hyperresponsiveness to methacholine after single exposure to aerosolized antigen in mice. *J Clin Invest.* 1998;101(8):1614–1622.
79. Presland RB, Boggess D, Lewis SP, Hull C, Fleckman P, Sundberg JP. Loss of normal profilaggrin and filaggrin in flaky tail (ft/ft) mice: an animal model for the filaggrin-deficient skin disease ichthyosis vulgaris. *J Invest Dermatol.* 2000;115(6):1072–1081.
80. Sundberg JP. The flaky tail (ft) mutation. In: Sundberg JP, ed. *Handbook of Mouse Mutations with Skin and Hair Abnormalities. Animal Models and Biochemical Tools*. Vol. 2. Ann Arbor, Michigan, USA: CRC Press; 1984:269–273.
81. Fallon PG, et al. A homozygous frameshift mutation in the mouse Flg gene facilitates enhanced percutaneous allergen priming. *Nat Genet.* 2009;41(5):602–608.
82. Scharschmidt TC, et al. Filaggrin deficiency confers a paracellular barrier abnormality that reduces inflammatory thresholds to irritants and haptens. *J Allergy Clin Immunol.* 2009;124(3):496–506.
83. Moniaga CS, et al. Flaky tail mouse denotes human atopic dermatitis in the steady state and by topical application with Dermatophagoides pteronyssinus extract. *Am J Pathol.* 2010;176(5):2385–2393.
84. Deraison C, et al. LEKTI fragments specifically inhibit KLK5, KLK7, and KLK14 and control desquamation through a pH-dependent interaction. *Mol Biol Cell.* 2007;18(9):3607–3619.
85. Ovaere P, Lippens S, Vandenabeele P, Declercq W. The emerging roles of serine protease cascades in the epidermis. *Trends Biochem Sci.* 2009;34(9):453–463.
86. Walley AJ, et al. Gene polymorphism in Netherton and common atopic disease. *Nat Genet.* 2001;29(2):175–178.
87. Kato A, Fukai K, Oiso N, Hosomi N, Murakami T, Ishii M. Association of SPINK5 gene polymorphisms with atopic dermatitis in the Japanese population. *Br J Dermatol.* 2003;148(4):665–669.
88. Nishio Y, et al. Association between polymorphisms in the SPINK5 gene and atopic dermatitis in the Japanese. *Genes Immun.* 2003;4(7):515–517.
89. Chavanas S, et al. Mutations in SPINK5, encoding a serine protease inhibitor, cause Netherton syndrome. *Nat Genet.* 2000;25(2):141–142.
90. Frenk E, Mevorah B. Ichthyosis linearis circumflexa Comèl with Trichorrhexis invaginata (Netherton's Syndrom): an ultrastructural study of the skin changes. *Arch Dermatol Forsch.* 1972;245(1):42–49.
91. Fartasch M, Williams ML, Elias PM. Altered lamellar body secretion and stratum corneum membrane structure in Netherton syndrome: differentiation from other infantile erythrodermas and pathogenic implications. *Arch Dermatol.* 1999;135(7):823–832.
92. Müller FB, et al. Genetic analysis of a severe case of Netherton syndrome and application for prenatal testing. *Br J Dermatol.* 2002;146(3):495–499.
93. Yang T, Liang D, Koch PJ, Hohl D, Kheradmand F, Overbeek PA. Epidermal detachment, desmosomal dissociation, and destabilization of corneodesmosin in Spink5$^{-/-}$ mice. *Genes Dev.* 2004; 18(19):2354–2358.
94. Descargues P, et al. Spink5-deficient mice mimic Netherton syndrome through degradation of desmoglein 1 by epidermal protease hyperactivity. *Nat Genet.* 2005;37(1):56–65.
95. Descargues P, et al. Corneodesmosomal cadherins are preferential targets of stratum corneum trypsin- and chymotrypsin-like hyperactivity in Netherton syndrome. *J Invest Dermatol.* 2006;126(7):1622–1632.
96. Vasilopoulos Y, et al. Genetic association between an AACC insertion in the 3'UTR of the stratum corneum chymotryptic enzyme gene and atopic dermatitis. *J Invest Dermatol.* 2004;123(1):62–66.
97. Oji V, et al. Loss of corneodesmosin leads to severe skin barrier defect, pruritus, and atopy: unraveling the peeling skin disease. *Am J Hum Genet.* 2010;87(2):274–281.
98. Bonnart C, et al. Elastase 2 is expressed in human and mouse epidermis and impairs skin barrier function in Netherton syndrome through filaggrin and lipid misprocessing. *J Clin Invest.* 2010;120(3):871–882.
99. Matsui T, et al. Skin-specific aspartic protease SASPase regulate stratum corneum hydration through profilaggrin processing. *EMBO Mol Med.* 2011;3(6):320–333.
100. Denecker G, et al. Caspase-14 protects against epidermal UVB photodamage and water loss. *Nat Cell Biol.* 2007;9(6):666–674.
101. Hoste E, et al. Caspase-14 is required for filaggrin degradation to natural moisturizing factors in the skin [published online ahead of print June 9, 2011]. *J Invest Dermatol.* doi:10.1038/jid.2011.153.
102. Kamata Y, et al. Neutral cysteine protease bleomycin hydrolase is essential for the breakdown of deiminated filaggrin into amino acids. *J Biol Chem.* 2009;284(19):12829–12836.
103. Kamata Y, et al. Bleomycin hydrolase is regulated biphasically in a differentiation- and cytokine-dependent manner: relevance to atopic dermatitis. *J Biol Chem.* 2011;286(10):8204–8212.
104. Schwartz DR, Homanics GE, Hoyt DG, Klein E, Abernethy J, Lazo JS. The neutral cysteine protease bleomycin hydrolase is essential for epidermal integrity and bleomycin resistance. *Proc Natl Acad Sci U S A.* 1999;96(8):4680–4685.
105. Morita K, et al. Molecular architecture of tight junctions of periderm differs from that of the maculae occludentes of epidermis. *J Invest Dermatol.* 2002;118(6):1073–1079.
106. Turksen K, Troy T-C. Permeability barrier dysfunction in transgenic mice overexpressing claudin 6. *Development.* 2002;129(7):1775–1784.
107. Hadj-Rabia S, et al. Claudin-1 gene mutations in neonatal sclerosing cholangitis associated with ichthyosis: a tight junction disease. *Gastroenterology.* 2004;127(5):1386–1390.
108. Feldmeyer L, Huber M, Fellmann F, Beckmann JS, Frenk E, Hohl D. Confirmation of the origin of NISCH syndrome. *Hum Mutat.* 2006;27(5):408–410.
109. De Benedetto A, et al. Tight junction defects in patients with atopic dermatitis. *J Allergy Clin Immunol.* 2011;127(3):773–786.
110. Uitto J, McGrath JA, Rodeck U, Bruckner-Tuderman L, Robinson EC. Progress in epidermolysis bullosa research: toward treatment and cure. *J Invest Dermatol.* 2010;130(7):1778–1784.
111. Wan H, et al. Der p 1 facilitates transepithelial allergen delivery by disruption of tight junctions. *J Clin Invest.* 1999;104(1):123–133.
112. Hammad H, Chieppa M, Perros F, Willart MA, Germain RN, Lambrecht BN. House dust mite allergen induces asthma via Toll-like receptor 4 triggering of airway structural cells. *Nat Med.* 2009; 15(4):410–416.
113. Kato T, et al. Mite serine protease activates protease-activated receptor-2 and induces cytokine release in human keratinocytes. *Allergy.* 2009; 64(9):1366–1374.
114. Vu AT, et al. Staphylococcus aureus membrane and diacylated lipopeptide induce thymic stromal lymphopoietin in keratinocytes through the Toll-like receptor 2-Toll-like receptor 6 pathway. *J Allergy Clin Immunol.* 2010;126(5):985–993.
115. Kim BE, et al. TNF-alpha downregulates filaggrin and loricrin through c-Jun N-terminal kinase: role for TNF-alpha antagonists to improve skin barrier. *J Invest Dermatol.* 2011;131(6):1272–1279.
116. Howell MD, et al. Cytokine modulation of atopic dermatitis filaggrin skin expression. *J Allergy Clin Immunol.* 2007;120(1):150–155.
117. Gutowska-Owsiak D, Schaupp AL, Salimi M, Taylor S, Ogg GS. Interleukin-22 downregulates filaggrin expression and affects expression of profilaggrin processing enzymes. *Br J Dermatol.* 2011; 165(3):492–498.
118. Hvid M, Vestergaard C, Kemp K, Christensen GB, Deleuran B, Deleuran M. IL-25 in atopic dermatitis: a possible link between inflammation and skin barrier dysfunction? *J Invest Dermatol.* 2011;131(1):150–157.
119. Hvid M, Johansen C, Deleuran B, Kemp K, Deleuran M, Vestergaard C. Regulation of caspase 14 expression in keratinocytes by inflammatory cytokines - a possible link between reduced skin barrier function and inflammation? *Exp Dermatol.* 2011;20(8):633–636.
120. Ozcan E, Notarangelo LD, Geha RS. Primary immune deficiencies with aberrant IgE production. *J Allergy Clin Immunol.* 2008;122(6):1054–1062.
121. Lesiak A, et al. Combined occurrence of filaggrin mutations and IL-10 or IL-13 polymorphisms predisposes to atopic dermatitis. *Exp Dermatol.* 2011;20(6):491–495.
122. Simpson EL, Berry TM, Brown PA, Hanifin JM. A pilot study of emollient therapy for the primary prevention of atopic dermatitis. *J Am Acad Dermatol.* 2010;63(4):587–593.
123. Stefansson K, et al. Activation of proteinase-activated receptor-2 by human kallikrein-related peptidases. *J Invest Dermatol.* 2008;128(1):18–25.
124. Enk AH, Angeloni VL, Udey MC, Katz SI. An essential role for Langerhans cell-derived IL-1 beta in the initiation of primary immune responses in skin. *J Immunol.* 1993;150(9):3698–3704.
125. Vasilopoulos Y, et al. A nonsynonymous substitution of cystatin A, a cysteine protease inhibitor of house dust mite protease, leads to decreased mRNA stability and shows a significant association with atopic dermatitis. *Allergy.* 2007;62(5):514–519.
126. Hubiche T, et al. Analysis of SPINK 5, KLK 7 and FLG genotypes in a French atopic dermatitis cohort. *Acta Dermato-Venereologica.* 2007;87(6):499–505.

Altered stratum corneum barrier and enhanced percutaneous immune responses in filaggrin-null mice

Hiroshi Kawasaki, MD,[a] Keisuke Nagao, MD, PhD,[a] Akiharu Kubo, MD, PhD,[a,b] Tsuyoshi Hata, PhD,[a,c] Atsushi Shimizu, DVM, PhD,[a] Hideaki Mizuno, PhD,[d] Taketo Yamada, MD, PhD,[e] and Masayuki Amagai, MD, PhD[a] *Tokyo and Wako, Japan*

Background: Loss-of-function mutations in filaggrin are major predisposing factors for atopic dermatitis. Although various reports suggest a critical role for filaggrin in stratum corneum (SC) barrier formation, the lack of filaggrin-null ($Flg^{-/-}$) mice has hampered detailed *in vivo* analysis of filaggrin's functions.
Objective: We sought to generate $Flg^{-/-}$ mice and to assess the effect of filaggrin loss on SC barrier function and percutaneous immune responses.
Methods: We generated $Flg^{-/-}$ mice using gene targeting and assessed the morphology, hydration, mechanical strength, and antigen permeability of their SC. Percutaneous immune responses were evaluated through irritant- and hapten-induced contact hypersensitivity studies and by measuring humoral responses to epicutaneous sensitization with protein antigen.
Results: Newborn $Flg^{-/-}$ mice exhibited dry scaly skin. Despite marked decreases in natural moisturizing factor levels, which are filaggrin degradation products, SC hydration and transepidermal water loss were normal. Microscopic analyses suggested premature shedding of SC layers, and indeed, increased desquamation under mechanical stress was demonstrated. Loss of keratin patterns, which are critical for corneocyte stabilization, is likely attributable to fragility in the $Flg^{-/-}$ SC. Antigens penetrated the $Flg^{-/-}$ SC more efficiently, leading to enhanced responses in hapten-induced contact hypersensitivity and higher serum levels of anti-ovalbumin IgG_1 and IgE.
Conclusion: Complete filaggrin deficiency led to altered barrier integrity and enhanced sensitization, which are important factors in early-phase atopic dermatitis. $Flg^{-/-}$ mice should provide a valuable tool to further explore additional factors the dysfunction of which leads to uncontrolled inflammation in patients with atopic diseases. (J Allergy Clin Immunol 2012;129:1538-46.)

Key words: *Filaggrin, filaggrin-null mice, atopic dermatitis, ichthyosis vulgaris, barrier function, flaky tail mice, stratum corneum, percutaneous immune response*

The skin is a vital barrier that segregates living organisms from the external environment, thereby protecting them from a variety of physical insults.[1] The stratum corneum (SC) is the outermost layer of the epidermis and acts as the first line of defense. The SC is produced by a highly organized differentiation process in which keratinocytes in the basal layer of the epidermis move to the spinous and granular layers, ultimately forming a tough multilayer of corneocytes rich in intercellular lipids, such as ceramides, cholesterol, and free fatty acids.[2]

Filaggrin,[3] a major structural protein in the SC, is produced as the precursor profilaggrin.[4] Profilaggrin is the main constituent of keratohyalin granules in the granular layer (stratum granulosum [SG]) of the epidermis.[4] During the later stages of epidermal terminal differentiation, profilaggrin is dephosphorylated and proteolyzed into filaggrin monomers in the SG.[4] It has been shown that *in vitro* filaggrin monomers bind to and assemble keratin intermediate filaments, thereby generating macrofibrils.[3,5] Filaggrin is also postulated to contribute to the mechanical strength and integrity of the SC *in vivo*.[6] In the upper layers of the SC, filaggrin monomers are further processed to hygroscopic amino acids and their derivatives by proteases.[7] Together with chloride and sodium ions, lactate, and urea, filaggrin breakdown products form natural moisturizing factors (NMFs), which are believed to play a major role in SC hydration.[8] Although circumstantial evidence suggests that filaggrin is crucial for maintaining SC integrity, its detailed mechanisms and *in vivo* roles remain elusive.

Recently, loss-of-function mutations in the filaggrin gene *(FLG)* were reported to cause ichthyosis vulgaris (IV),[9] a common autosomal dominant keratinization disorder characterized by scaly skin, and were further identified as major predisposing factors for atopic dermatitis (AD).[10,11] AD is a chronic skin disorder characterized by dry skin and eczema and is frequently associated with increased serum IgE levels and a personal or family history of AD, allergic rhinitis, and/or asthma.[12] It has been hypothesized that SC barrier disruption caused by filaggrin deficiency is the primary event in AD, allowing antigen penetration and percutaneous sensitization, followed by allergic responses

From [a]the Department of Dermatology, [b]the Center for Integrated Medical Research, and [e]the Department of Pathology, Keio University School of Medicine, Tokyo; [c]Fundamental Research Laboratories, KOSÉ Corporation, Tokyo; and [d]the Brain Science Institute, RIKEN, Wako.

Supported by a Health Labour Sciences Research Grant for Research on Allergic Diseases and Immunology from the Ministry of Health, Labour and Welfare of Japan; Grants-in-Aid for Scientific Research; the "Promotion of Environmental Improvement for Independence of Young Researchers" program and a Matching Fund Subsidy for Private Universities from the Ministry of Education, Culture, Sports, Science and Technology of Japan; Research Grants for Life Sciences and Medicine from Keio University Medical Science Fund; and a Keio University Grant-in-Aid for Encouragement of Young Medical Scientists.

Disclosure of potential conflict of interest: The authors declare that they have no relevant conflicts of interest.

Received for publication September 18, 2011; revised January 24, 2012; accepted for publication January 25, 2012.

Available online March 10, 2012.

Corresponding author: Masayuki Amagai, MD, PhD, Department of Dermatology, Keio University School of Medicine, 35 Shinanomachi, Shinjyuku-ku, Tokyo, Japan. E-mail: amagai@a7.keio.jp.

0091-6749/$36.00

doi:10.1016/j.jaci.2012.01.068

Abbreviations used
AD: Atopic dermatitis
CHS: Contact hypersensitivity
DIA: Desquamation index for amount
DNFB: 1-Fluoro-2,4-dinitrobenzene
FLG: Human filaggrin gene
Flg: Murine filaggrin gene
ft/ma: Flaky tail/matted
IV: Ichthyosis vulgaris
NMF: Natural moisturizing factor
OVA: Ovalbumin
SC: Stratum corneum
SG: Stratum granulosum
SPF: Specific pathogen free
TEM: Transmission electron microscopy
TEWL: Transepidermal water loss
TS: Tape stripping
UTR: Untranslated region

to multiple environmental antigens.[13] Better understanding of filaggrin biology and the pathogenic effects of its loss would facilitate strategies for maintaining epidermal homeostasis.

Flaky tail/matted (ft/ma) mice experience spontaneous dermatitis with increased serum IgE levels[14,15] and carry a 1-bp deletional mutation (5303delA) in the murine filaggrin gene *(Flg)*.[16] ft/ma mice are commonly used to investigate pathogenic mechanisms of AD in the context of filaggrin deficiency.[14,15,17] However, they do not show complete loss of filaggrin, as discussed below. Together with the failure thus far to identify the gene responsible for the matted hair phenotype in ft/ma mice,[18-20] this limits the usefulness of ft/ma mice for investigating filaggrin function.

To address these issues and to improve understanding of SC function, we generated mice that were completely deficient in filaggrin. The functional properties of filaggrin-null ($Flg^{-/-}$) SC were characterized *in vitro* and *in vivo*, and percutaneous immune responses were assessed.

METHODS

Generation of $Flg^{-/-}$ mice

Flg, which is located on chromosome 3, consists of 3 exons and shares unique characteristics with its human counterpart. Exon 1 consists of 5′ untranslated region (UTR) sequences, exon 2 contains the translation start site, and the unusually large exon 3 encodes nearly identical filaggrin repeats (see Fig E1, *A*, in this article's Online Repository at www.jacionline.org). Large open reading frames and repetitive sequences complicate the strategy by which the genes are targeted. Nevertheless, we designed the targeting vector to remove both the start codon located in exon 2 and in-frame ATG sequences located at the 5′ end of exon 3, thereby excluding all of the in-frame ATG sequences in *Flg*. An ES cell clone was successfully obtained through homologous recombination between the targeting vector and *Flg*. The ES cell clone was injected into C57BL/6 blastocysts, and chimeric mice were produced. For details, see the Methods section in this article's Online Repository at www.jacionline.org.

Mice

$Flg^{-/-}$ and ft/ma mice (The Jackson Laboratory, Bar Harbor, Me) were backcrossed 6 generations onto C57BL/6 and BALB/c (CLEA Japan, Inc, Tokyo, Japan) backgrounds by using the speed congenic services of the Central Institute for Experimental Animals (Kawasaki, Japan), and greater than 99% recipient genome content was confirmed. All mice were maintained under specific pathogen-free (SPF) conditions, and all procedures were approved by the Keio University Ethics Committee for Animal Experiments. Experiments regarding SC barrier functions were performed under normal, unmanipulated housing conditions. For more information, see the Methods section in this article's Online Repository at www.jacionline.org.

Percutaneous immune responses

To assess irritant contact dermatitis, 20 μL of croton oil (0.6%; Sigma-Aldrich, St Louis, Mo) in acetone/olive oil (4:1) was applied once to the inner and outer surfaces of the ear. To evaluate hapten-induced contact hypersensitivity (CHS) responses, 25 μL of 0.5% 1-fluoro-2,4-dinitrobenzene (DNFB; Nacalai Tesque, Kyoto, Japan) in acetone/olive oil (4:1) was applied (for sensitization) to the shaved abdomens of mice, which were challenged with 20 μL of 0.3% DNFB (applied to the ear) 5 days later. Changes in ear thickness were measured at specific subsequent time points by using a thickness gauge (Teclock PG-20, Nagano, Japan).

To analyze the humoral responses to percutaneously applied protein antigen, we applied 10 μL of 2 mg/mL ovalbumin (OVA; Sigma-Aldrich) and 10 μL of dibutyl phthalate to the ears of mice 8 times every other day. OVA-specific serum IgG_1 and IgE levels were detected 1 week after the final application. Serum antibody analysis is described in the Methods section in this article's Online Repository.

Statistical analysis

All experiments were analyzed by using the 2-tailed Student *t* test or ANOVA with GraphPad Prism 5.0 software (GraphPad Software, Inc, San Diego, Calif). All results are presented as means ± SEMs. A P value of less than .05 was considered significant.

RESULTS

Generation of $Flg^{-/-}$ mice

$Flg^{-/-}$ mice were generated by means of homologous recombination (see the Methods section and Fig E1 in this article's Online Repository). Mice were backcrossed to both C57BL/6 and BALB/c backgrounds to minimize phenotypic variation. Immunoblotting and immunohistochemical analyses revealed that *Flg*-targeted mice were completely deficient for both profilaggrin and filaggrin (Fig 1), which is in contrast to ft/ma mice, in which abundant amounts of truncated profilaggrin and low but detectable levels of mature filaggrin were demonstrated through Western blotting (Fig 1, *A*, and see the Methods section in this article's Online Repository). Immunohistochemical staining in ft/ma mice also reproducibly revealed positive filaggrin staining at lower levels than in wild-type skin. Thus despite their use as a model of filaggrin deficiency,[14-17] ft/ma mice do not display complete loss of filaggrin. Results in the context of filaggrin function or deficiency obtained with these mice must be interpreted carefully. Levels of the epidermal differentiation markers involucrin and loricrin, as well as keratin 1, which is expressed in the spinous and granular layers of the epidermis, were unaffected by the loss of filaggrin (Fig 1).

$Flg^{-/-}$ mice have dry scaly skin

$Flg^{-/-}$ mice were viable and healthy, with no apparent growth restriction. Although $Flg^{-/-}$ mice and wild-type littermates were macroscopically indistinguishable immediately after birth, differences became evident between days 3 and 6 after birth. Compared with wild-type littermates, neonatal $Flg^{-/-}$ mice

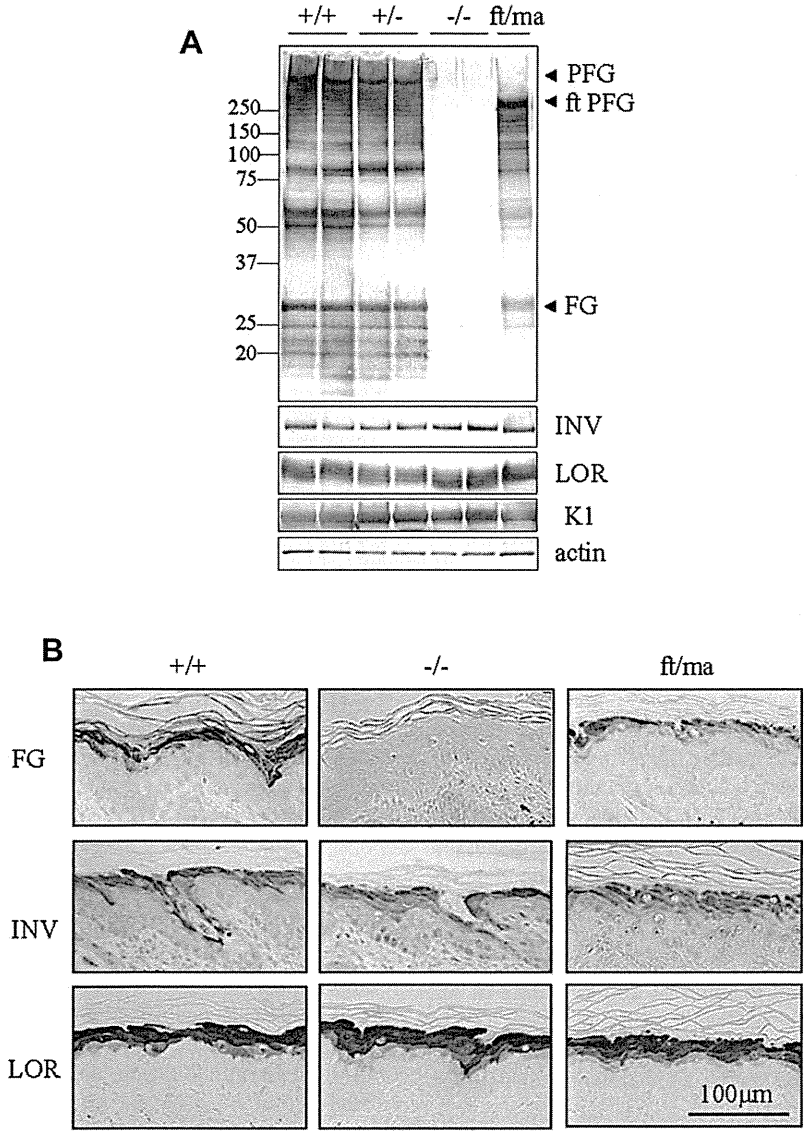

FIG 1. Loss of filaggrin expression in $Flg^{-/-}$ mice. **A,** Western blot analysis of urea/Tris extracts from wild-type *(+/+)*, heterozygous *(+/−)*, and $Flg^{-/-}$ *(−/−)* mice and 5-day-old ft/ma littermates. *Left,* Molecular weight marker sizes (in kilodaltons). **B,** Immunohistochemical staining of wild-type, $Flg^{-/-}$, and ft/ma dorsal skin on day 4. *FG,* Filaggrin; *ft PFG,* ft/ma mutant profilaggrin; *INV,* involucrin; *K1,* keratin 1; *LOR,* loricrin; *PFG,* profilaggrin.

exhibited dry scaly skin with a shiny tone and prominent areas of crista cutis surrounded by deep furrows (Fig 2, *A* and *B*). Light microscopic examination of hematoxylin and eosin–stained neonatal and adult $Flg^{-/-}$ murine sections showed markedly fewer keratohyalin granules in the SG but showed no apparent abnormalities in the lower layers (Fig 2, *C*, adult mice; data not shown). Both $Flg^{-/-}$ and wild-type mice had normal hair growth, and the trunk skin phenotype of $Flg^{-/-}$ mice became less obvious after hair outgrowth. Dry scaly skin was repeatedly observed on the tails, perhaps because of the low hair density, and this was typically most prominent in 2- to 3-week-old $Flg^{-/-}$ mice. Such lesions displayed compact hyperkeratosis in histologic analyses (Fig 2, *D* and *E*). Collectively, $Flg^{-/-}$ mice exhibited dry scaly skin with abnormal keratosis, a phenotype consistent with the features of human IV, an inherited disease caused by filaggrin deficiency.

Dry skin in $Flg^{-/-}$ mice is unrelated to SC water content and transepidermal water loss

To determine whether the dry scaly skin phenotype in $Flg^{-/-}$ mice was attributable to SC moisturizing states, we evaluated NMF and water profiles. It has been reported that filaggrin is essential for SC hydration, with filaggrin-derived NMFs being a source of hygroscopic amino acids.[8] As expected, amino acid levels in $Flg^{-/-}$ SC were reduced (Fig 3, *A*). *In vivo* confocal Raman microspectroscopic analysis consistently showed reduced NMF levels, which is in agreement with recent human reports on patients with *FLG* mutations (Fig 3, *B*).[21,22]

The loss of NMFs was expected to lead to reduced water content. Interestingly, however, *in vivo* confocal Raman microspectroscopy analysis revealed normal SC water levels in $Flg^{-/-}$ mice (Fig 3, *C*). Measurement of skin conductance yielded similar results (Fig 3, *D*). These observations demonstrate that NMFs

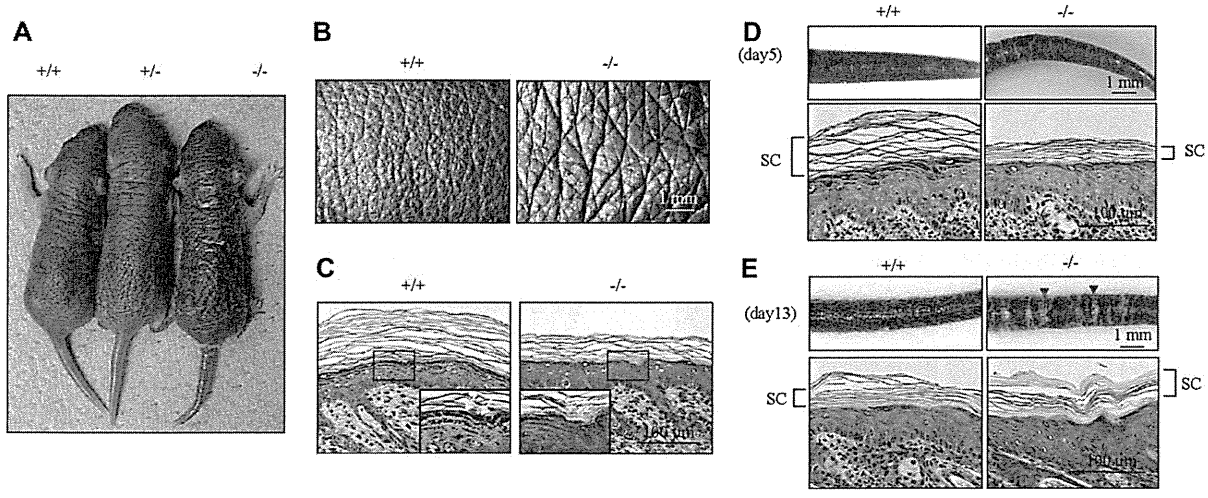

FIG 2. *Flg*$^{-/-}$ mice exhibit an ichthyotic skin phenotype. **A-C,** Macroscopic (Fig 2, *A*), negative replica (Fig 2, *B*), and histologic (hematoxylin and eosin staining; Fig 2, *C*) images of neonatal *Flg*$^{-/-}$ mice. *Insets,* Higher-magnification images of the highlighted areas. *Arrows,* Keratohyalin granules. **D** and **E,** Macroscopic *(upper panel)* and histologic *(lower panel)* images of tail skin from wild-type *(+/+)* and *Flg*$^{-/-}$ *(−/−)* mice on days 4 (Fig 2, *D*) and 13 (Fig 2, *E*). *Arrowheads,* Scale.

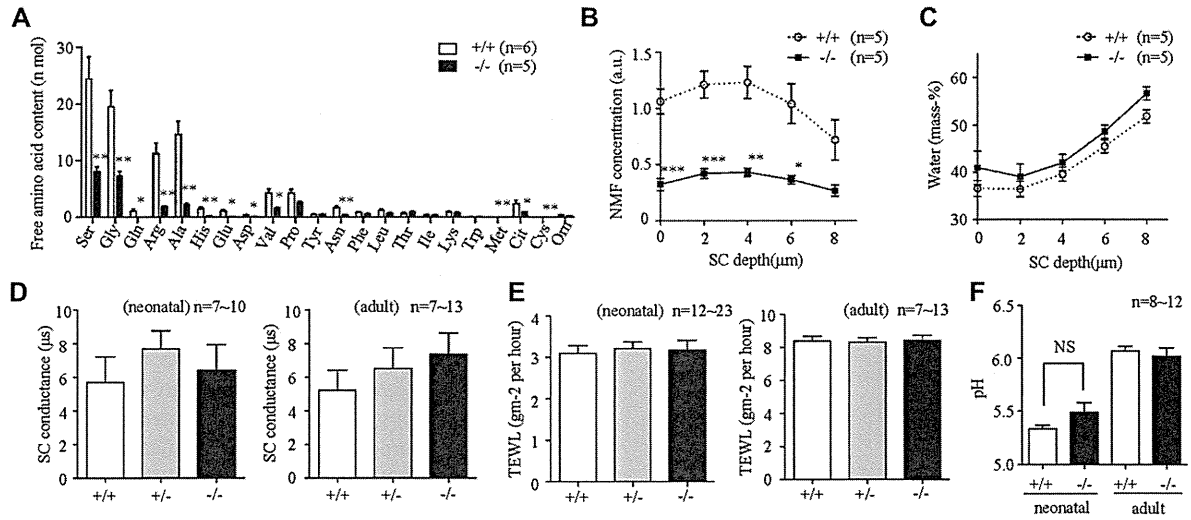

FIG 3. Decreased *in vivo* NMF levels and normal water content and TEWL in *Flg*$^{-/-}$ SC. **A,** Free amino acid content in the SC of neonatal wild-type *(+/+)* and *Flg*$^{-/-}$ *(−/−)* mice. **B** and **C,** Dorsal skin NMF concentration (Fig 3, *B*) and relative water profiles (Fig 3, *C*) were measured *in vivo* by using confocal Raman microspectroscopy. **D-F,** Comparison of TEWL (Fig 3, *D*), SC hydration (Fig 3, *E*), and SC surface pH (Fig 3, *F*) between neonatal and adult wild-type, heterozygous *(+/−)*, and *Flg*$^{-/-}$ mice. *NS,* Not significant. **P* < .05, ***P* < .01, and ****P* < .001.

derived from filaggrin did not primarily function to maintain SC hydration in the steady state.

We further analyzed transepidermal water loss (TEWL). It is generally agreed that TEWL correlates with the amount of water that evaporates from the body surface and that increased TEWL is indicative of SC barrier dysfunction.[23] TEWL is thus used as a surrogate marker to assess skin dryness and SC barrier function in patients with AD.[23] In agreement with the water content observations and despite their dry skin appearances, both neonatal and adult *Flg*$^{-/-}$ mice displayed unaltered TEWL values (Fig 3, *E*). In addition, filaggrin deficiency has been described to result in increased pH in the SC,[2] followed by abnormal activities of multiple enzymes in the SC that act pH-dependently, finally leading to SC barriers with abnormal function. Analysis in *Flg*$^{-/-}$ mice, however, demonstrated that filaggrin deficiency did not affect SC surface pH during evaluated time points (Fig 3, *F*), demonstrating that the above aberrant cascade does not occur. This is consistent with the recent report that filaggrin is not essential for SC accidification.[24] Therefore filaggrin deficiency does not directly affect hydration status or pH in the SC.

Flg$^{-/-}$ SC is prone to desquamation under mechanical stress

To further investigate the effect of filaggrin deficiency, we assessed skin surface morphology in *Flg*$^{-/-}$ mice by using

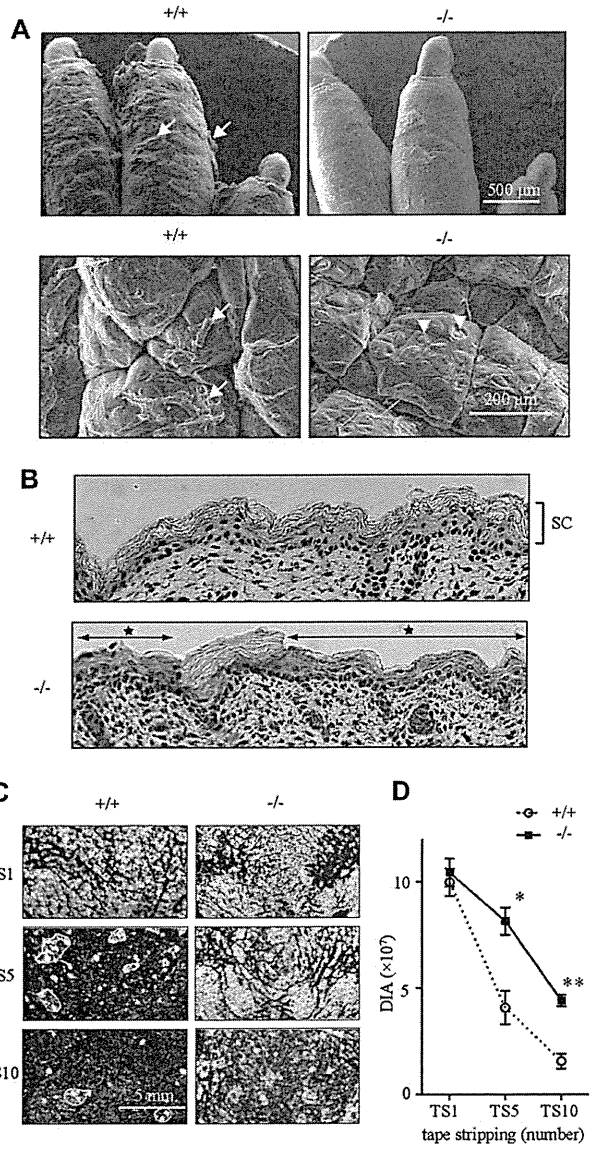

FIG 4. Filaggrin-deficient SC is fragile and more susceptible to TS. **A,** Low-vacuum scanning electron microscopic images of paws *(upper panel)* and abdominal skin *(lower panel).* **B,** Histologic images of the SC layers. **C** and **D,** Evaluation of SC fragility by using TS. *Arrows,* Cornified materials; *arrowheads,* nuclei of cells in viable layers. +/+, Wild-type mice; −/−, $Flg^{-/-}$ mice. $*P < .05$ and $**P < .01$.

low-vacuum scanning electron microscopy. We found that whereas the paw skin of wild-type mice was covered with ribbons of cornified material, that of $Flg^{-/-}$ mice was not (Fig 4, *A*). Similarly, focal areas of the crista cutis in abdominal skin lacked these ribbons, where nuclei appeared to be visible in cells of viable layers just below the SC (Fig 4, *A*). Such observations were never made in wild-type animals. Safranin staining of SC layers revealed focal areas of SC defects in $Flg^{-/-}$ mice (Fig 4, *B*, star) but not in wild-type littermates (Fig 4, *B*).

This observation led us to hypothesize that premature detachment of cornified layers might occur in $Flg^{-/-}$ SC and that the SC might be prone to desquamation under mechanical stress. To address this question, we performed carefully controlled tape-stripping (TS) experiments in neonatal mice (see the Methods section in this article's Online Repository). TS once (TS1) resulted in uniform detachment of cornified materials from the skin surface. The amount of detached cornified materials attached to the tape was evaluated by calculating the desquamation index for amount (DIA), and repeating this assay at the same sites allowed assessment of vulnerability of the SC to mechanical stress. TS1 in wild-type and $Flg^{-/-}$ mice yielded equal DIA values (Fig 4, *C* and *D*). However, after 5 (TS5) and 10 (TS10) rounds of TS, DIA values were significantly higher in $Flg^{-/-}$ mice than in wild-type mice, indicating that whereas the deeper layers of the wild-type SC were resistant to mechanical stress, those of $Flg^{-/-}$ mice were prone to detach prematurely and were therefore more fragile.

Abnormal keratin filament aggregation in $Flg^{-/-}$ mice

Filaggrin promotes keratin filament aggregation[3,5] and is believed to contribute to the mechanical strength and integrity of the SC.[6] We therefore assessed whether SC fragility in $Flg^{-/-}$ mice was actually associated with abnormal keratin filament aggregation. Conventional transmission electron microscopic (TEM) analysis of wild-type and $Flg^{-/-}$ mice revealed a normal distribution and number of desmosomes, suggesting that cell-cell adhesion was unimpaired (Fig 5, *A*, asterisk). However, close observation revealed that the keratohyalin granules (Fig 5, *A*, KGs) were disorganized and that bundles of keratin filaments were immature and did not establish a robust network of filaments extending to desmosomes in the upper parts of the SG (Fig 5, *A*).

Keratin patterns represent densely packed keratin filaments,[3,5,25,26] and extensive cryoelectron TEM has led to the establishment of the "cubic rod-packing" model in which rods of keratin filaments are 3-dimensionally interlaced in a hexagonal pattern to yield the stiffest possible corneocyte keratin framework.[27] Examination of wild-type and $Flg^{-/-}$ SC samples post-fixed with ruthenium tetroxide revealed beautifully interlaced keratin in corneocytes in the lower 3 to 4 layers of the wild-type SC. In striking contrast, keratin intermediate filaments in lower SC layer corneocytes in $Flg^{-/-}$ mice were not interlaced, and their keratin patterns were abolished (Fig 5, *B*). This loss of keratin patterns could well alter SC integrity and lead to enhanced susceptibility to mechanical stress in $Flg^{-/-}$ mice. Corneodesmosomes, lamellar body secretion, and extracellular lamellar bilayers at the SG-SC interface appeared to be unaffected by filaggrin deficiency (Fig 5, *C* and *D*).

Increased penetration of foreign materials in $Flg^{-/-}$ mice

We next assessed whether filaggrin deficiency affected the ability of foreign material to permeate the SC, a relevant question in the context of AD. To address this issue, solutions of unmodified or liposome-encapsulated calcein, a fluorescent substance, were topically applied to tail skin of adult mice, and permeability was evaluated by means of confocal microscopic analysis of cryosections with, for accurate evaluation, the Kawamoto film method (with modifications), which prevents the diffusion of fluorescence and preserves tissue components during sample preparation (see the Methods section in this article's Online Repository).[28] No fluorescence signal was detected in $Flg^{-/-}$ or wild-type SC from mice treated with unmodified calcein aqueous

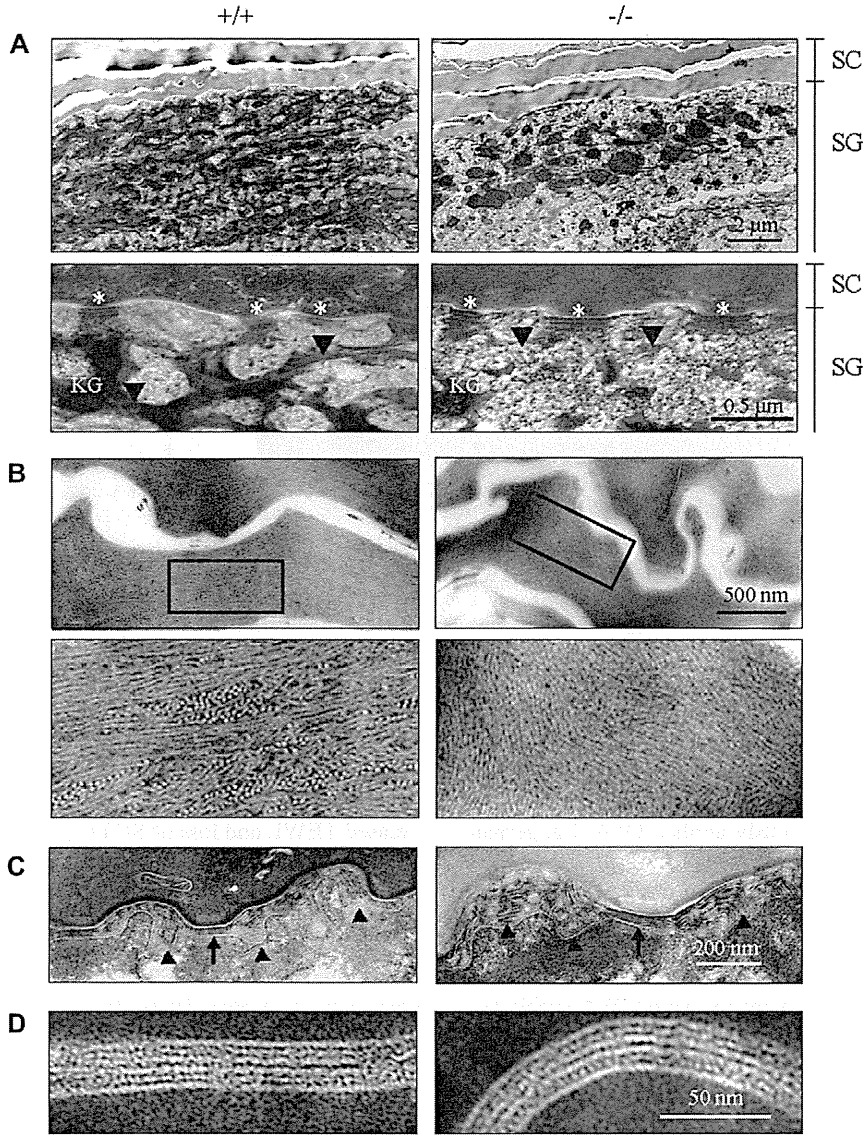

FIG 5. Abnormal keratin filament aggregation in $Flg^{-/-}$ epidermis. **A,** Disorganized keratohyaline granules *(KG)* and immature bundles of keratin filaments *(arrowheads)* in $Flg^{-/-}$ SG. *Asterisks,* Desmosome. **B,** Disturbed keratin intermediate filament organization in $Flg^{-/-}$ SC. *Lower panels,* Higher-magnification images of the highlighted areas. **C** and **D,** Lamellar body secretion *(arrowheads),* corneodesmosomes (*arrows*; Fig 5, *C*), and extracellular lamellar bilayers (Fig 5, D) at the SG-SC interface appeared normal in $Flg^{-/-}$ *(−/−)* mice. +/+, Wild-type mice.

solution (Fig 6, *A* and *B*). Interestingly, however, calcein encapsulated in liposomes penetrated $Flg^{-/-}$ but not wild-type SC. Focal areas with fluorescent signals were regularly found throughout $Flg^{-/-}$ SC (Fig 6, *C* and *D*). These results demonstrate an important role for filaggrin in maintaining SC integrity and thereby preventing the penetration of this barrier by allergens. Although further definitive clarification requires further studies, the ability of topically applied substances to permeate $Flg^{-/-}$ SC appears to be affected by the solvent in which they are dissolved.

Enhanced percutaneous immune responses in $Flg^{-/-}$ mice

Long-term observations revealed that $Flg^{-/-}$ mice on both the C57BL/6 and BALB/c backgrounds did not have spontaneous dermatitis under SPF conditions (see Fig E2 in this article's Online Repository at www.jacionline.org), suggesting that exposure to environmental factors might be a critical factor. To characterize percutaneous immune responses to exogenous substances under filaggrin-deficient conditions, we evaluated $Flg^{-/-}$ mice in irritant and allergic contact dermatitis models. When croton oil was topically applied to murine ears to cause irritant contact dermatitis, $Flg^{-/-}$ mice exhibited enhanced ear-swelling responses throughout the experimental period, indicating that $Flg^{-/-}$ SC allows this irritant to reach the viable layers to a greater extent than wild-type SC (Fig 7, *A*).

Hapten (DNFB)–induced CHS was used to evaluate cellular immune responses. Ear thickness was significantly increased in $Flg^{-/-}$ mice (Fig 7, *B*) compared with that seen in wild-type and nonimmunized $Flg^{-/-}$ mice. Histologic analysis revealed greater

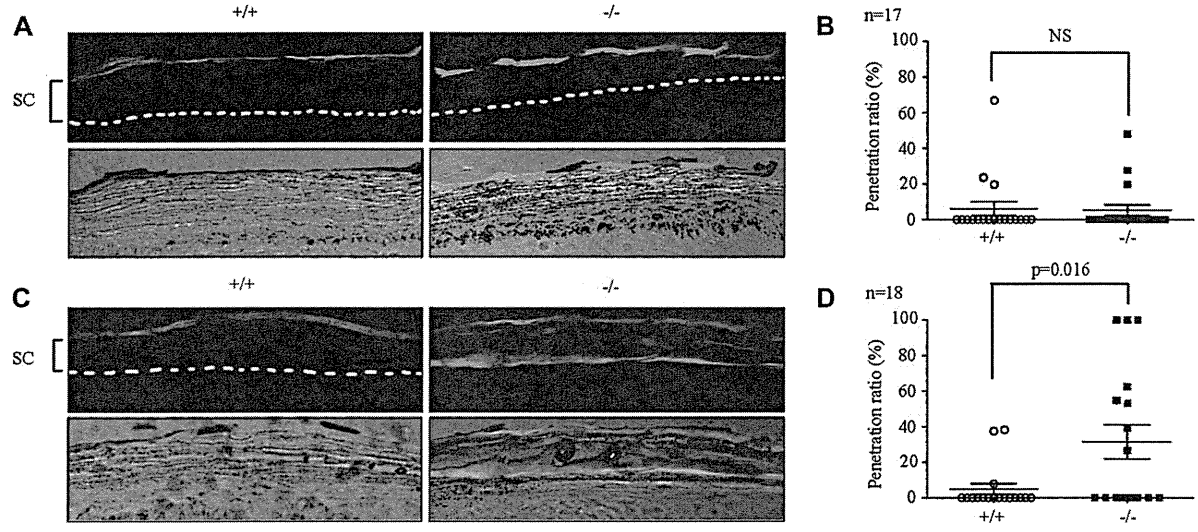

FIG 6. Increased penetration of foreign materials in $Flg^{-/-}$ mice. **A** and **C,** Calcein solution (Fig 6, *A*) and calcein encapsulated in liposomes (Fig 6, *C*) were topically applied to the tails of 8-week-old mice, and permeability was examined with confocal microscopy. **B** and **D,** Penetration ratio: the proportion of fluorescence that penetrated more than half of the SC. *Dashed white lines,* Border between the SC and SG. +/+, Wild-type mice; −/−, $Flg^{-/-}$ mice; *NS,* not significant.

edema and inflammation (Fig 7, *C*), indicating that $Flg^{-/-}$ mice exhibited exaggerated irritant and allergic contact dermatitis responses.

These results prompted us to evaluate protein antigen-specific humoral responses to percutaneously applied OVA. Langerhans cells have been shown to be capable of capturing protein antigens that exist outside epidermal tight junction barriers[29,30] and then elicit T_H2 humoral responses *in vivo*.[30,31] Because topical application of OVA alone did not elicit a response, we repeatedly applied OVA with dibutyl phthalate, which is reported to be a T_H2 adjuvant,[32] to the ear skin of mice and measured OVA-specific serum antibody levels. Concordant with the hapten-induced CHS results, IgG_1 and IgE responses to OVA were enhanced in $Flg^{-/-}$ mice (Fig 7, *D*), demonstrating exaggerated T_H2 humoral responses in the absence of filaggrin. Collectively, our results suggest that alterations in the SC barrier in $Flg^{-/-}$ mice allowed penetration of irritants, haptens, and protein antigens and led to exaggerated responses in the context of irritant contact dermatitis and T_H1 and T_H2 immune responses.

DISCUSSION

Filaggrin has been demonstrated to function in SC integrity as a structural protein that organizes keratin filaments.[6] It is also a major source of the hygroscopic amino acids in SC referred to as NMFs.[8] NMFs are believed to maintain SC hydration levels.[8] Although the biology and functions of filaggrin have been modeled through *in vitro* experiments, its *in vivo* functions have remained elusive because of the absence of mice that completely and specifically lack filaggrin. This was due to technical difficulties in generating $Flg^{-/-}$ mice, which were attributed to the tandem repeats in *Flg* and complicated gene sequencing and targeting strategies. Given the growing importance of filaggrin in the context of AD, we successfully generated $Flg^{-/-}$ mice and used these mice to explore the role of filaggrin *in vivo*.

We unexpectedly observed that loss of NMFs as a result of filaggrin deficiency did not lead to decreased SC water content. Despite the dry appearance of their skin, $Flg^{-/-}$ mice exhibited normal SC hydration throughout their lives. It is interesting to compare $Flg^{-/-}$ mice with ft/ma mice, which have been reported to have spontaneous dermatitis (see Fig E2) and to display increased TEWL and loss of SC hydration,[14,17] which is consistent with findings in human AD (with and without *FLG* mutations).[33] We subsequently found that whereas TEWL and SC hydration were not impaired in ft/ma mice before the onset of dermatitis, TEWL increased and SC hydration decreased after these mice had dermatitis (see Fig E3 in this article's Online Repository at www.jacionline.org). These data indicate that increased TEWL and SC water loss in ft/ma mice are secondary to skin inflammation. Hydration of SC *in vivo* is also reported to be maintained by several other factors, such as intercellular lamellar lipids,[8] and is influenced by environmental aspects, such as humidity. The relation between filaggrin and SC hydration should be interpreted carefully.

Analyses of $Flg^{-/-}$ mice clearly demonstrated the important contribution of filaggrin to keratin filament network assembly *in vivo*. Filaggrin-deficient epidermis showed immature bundles and an aberrant network of keratin filaments in upper parts of the SG and loss of the keratin pattern in the lower SC. Interlaced keratin filaments form 3-dimensional lattice-like structures that physically stabilize the corneocyte keratin framework.[27] Loss of this interlaced keratin pattern in $Flg^{-/-}$ epidermis led to increased susceptibility to mechanical stress. Although it was previously found that some patients with IV display normal keratin patterns,[34,35] this likely depends on the mutation site and the extent of filaggrin loss.[36]

Events accompanying barrier dysfunction, in particular enhanced penetration by antigens and subsequent sensitization, are important immunologic steps in the pathogenesis of AD. In this study, evaluation of SC permeability revealed that $Flg^{-/-}$ skin exhibited enhanced penetration of liposome-encapsulated calcein throughout the SC layer in focal areas (Fig 6, *C* and *D*). This can be attributed to increased SC fragility and premature desquamation in $Flg^{-/-}$ mice. Interestingly, however, calcein

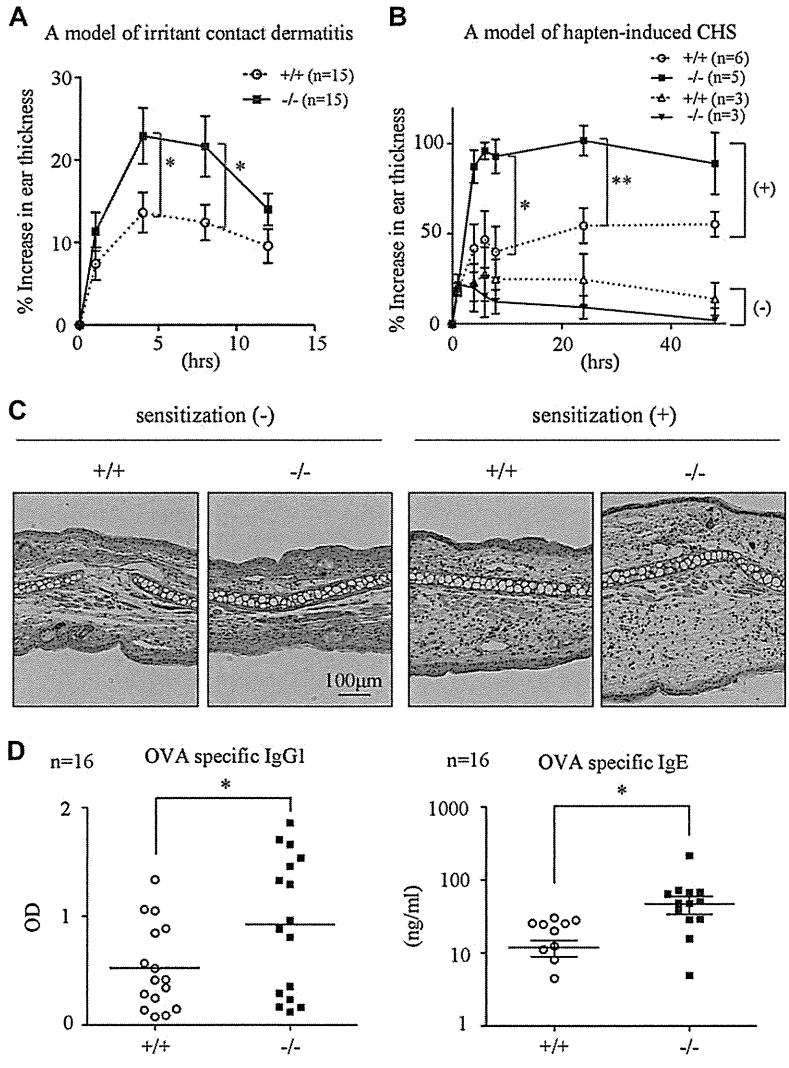

FIG 7. Enhanced percutaneous immune responses in $Flg^{-/-}$ mice. **A** and **B**, Percentage increase in ear thickness of mice after topical application of croton oil (Fig 7, *A*) and after DNFB challenge with *(+)* or without *(−)* sensitization (Fig 7, *B*). **C**, Histology after DNFB challenge. **D**, Systemic immune responses to repeated percutaneous application of OVA. OVA-specific serum IgG_1 and IgE levels were measured by using ELISA. +/+, Wild-type mice; −/−, $Flg^{-/-}$ mice. $*P < .05$ and $**P < .01$.

solubilized in water did not penetrate either wild-type or $Flg^{-/-}$ SC (Fig 6, *A* and *B*), indicating that the SC remained hydrophobic. It is of note that lipid composition was aberrant in $Flg^{-/-}$ SC, whereas free fatty acid levels remained normal, and levels of ceramide and cholesterol were increased (see the Methods section and Fig E4 in this article's Online Repository at www.jacionline.org). It is possible that aberrant lipid composition, as well as SC fragility, might have direct or indirect effects on the penetration of certain materials by affecting SC hydrophobicity.

Barrier disruption and continuous percutaneous exposure to allergens presumably initiate and drive AD. $Flg^{-/-}$ SC allowed the penetration of both hapten and protein antigens, which was followed by exaggerated immune responses. The ft/ma mice spontaneously have itchy skin lesions,[14,15] thus providing an attractive model for AD research. However, we showed that they do not completely lack filaggrin. This, together with the presence of the matted mutation, means that it is difficult to explore precise mechanisms of skin sensitization and dermatitis progression at the molecular level with ft/ma mice. Use of $Flg^{-/-}$ mice revealed that filaggrin was required for proper barrier formation *in vivo* and that its loss resulted in enhanced percutaneous cellular and humoral immune responses, which are important steps in the early phase of AD pathogenesis.

The insolubility of the SC has hampered progress in understanding its biology. Genetic ablation of relevant molecules *in vivo* is thus far the only method to overcome this issue. By generating $Flg^{-/-}$ mice, we demonstrated that filaggrin is necessary for proper barrier formation *in vivo*, with filaggrin deficiency leading to enhanced penetration of antigens and subsequent sensitization. Loss of or functional abnormalities in filaggrin is important in the early phase of AD development. Other environmental or genetic factors can be examined in these mice to further dissect SC biology *in vivo* and to explore other factors that contribute to prolonged and progressive dermatitis in the context of AD.

We thank Dr Akemi Ishida-Yamamoto and Dr Hiroyuki Sasaki for technical advice and technical support on TEM, Dr Tadafumi Kawamoto for technical assistance with the Kawamoto film method, and Mr Taizen Morishita for the

amino acid analysis. We also thank Ms Minae Suzuki for the preparation of frozen sections and Ms Hiromi Itoh for excellent animal care. Scanning electron microscopic analysis was a courtesy of Hitachi High-Technologies Corporation.

Clinical implications: The newly generated *Flg*$^{-/-}$ mice enabled the evaluation of filaggrin function *in vivo* and might be a highly useful tool for studying the epidermal barrier at the molecular level.

REFERENCES

1. Segre JA. Epidermal barrier formation and recovery in skin disorders. J Clin Invest 2006;116:1150-8.
2. Elias PM, Schmuth M. Abnormal skin barrier in the etiopathogenesis of atopic dermatitis. Curr Opin Allergy Clin Immunol 2009;9:437-46.
3. Steinert PM, Cantieri JS, Teller DC, Lonsdale-Eccles JD, Dale BA. Characterization of a class of cationic proteins that specifically interact with intermediate filaments. Proc Natl Acad Sci U S A 1981;78:4097-101.
4. Sandilands A, Sutherland C, Irvine AD, McLean WH. Filaggrin in the frontline: role in skin barrier function and disease. J Cell Sci 2009;122:1285-94.
5. Dale BA, Holbrook KA, Steinert PM. Assembly of stratum corneum basic protein and keratin filaments in macrofibrils. Nature 1978;276:729-31.
6. Dale BA, Resing KA, Lonsdale-Eccles JD. Filaggrin: a keratin filament associated protein. Ann N Y Acad Sci 1985;455:330-42.
7. Kamata Y, Taniguchi A, Yamamoto M, Nomura J, Ishihara K, Takahara H, et al. Neutral cysteine protease bleomycin hydrolase is essential for the breakdown of deiminated filaggrin into amino acids. J Biol Chem 2009;284:12829-36.
8. Rawlings AV, Harding CR. Moisturization and skin barrier function. Dermatol Ther 2004;17(suppl 1):43-8.
9. Smith FJ, Irvine AD, Terron-Kwiatkowski A, Sandilands A, Campbell LE, Zhao Y, et al. Loss-of-function mutations in the gene encoding filaggrin cause ichthyosis vulgaris. Nat Genet 2006;38:337-42.
10. Irvine AD. Fleshing out filaggrin phenotypes. J Invest Dermatol 2007;127:504-7.
11. Palmer CN, Irvine AD, Terron-Kwiatkowski A, Zhao Y, Liao H, Lee SP, et al. Common loss-of-function variants of the epidermal barrier protein filaggrin are a major predisposing factor for atopic dermatitis. Nat Genet 2006;38:441-6.
12. Bieber T. Atopic dermatitis. N Engl J Med 2008;358:1483-94.
13. McGrath JA, Uitto J. The filaggrin story: novel insights into skin-barrier function and disease. Trends Mol Med 2008;14:20-7.
14. Moniaga CS, Egawa G, Kawasaki H, Hara-Chikuma M, Honda T, Tanizaki H, et al. Flaky tail mouse denotes human atopic dermatitis in the steady state and by topical application with *Dermatophagoides pteronyssinus* extract. Am J Pathol 2010;176:2385-93.
15. Oyoshi MK, Murphy GF, Geha RS. Filaggrin-deficient mice exhibit TH17-dominated skin inflammation and permissiveness to epicutaneous sensitization with protein antigen. J Allergy Clin Immunol 2009;124:485-93, e1.
16. Fallon PG, Sasaki T, Sandilands A, Campbell LE, Saunders SP, Mangan NE, et al. A homozygous frameshift mutation in the mouse Flg gene facilitates enhanced percutaneous allergen priming. Nat Genet 2009;41:602-8.
17. Scharschmidt TC, Man MQ, Hatano Y, Crumrine D, Gunathilake R, Sundberg JP, et al. Filaggrin deficiency confers a paracellular barrier abnormality that reduces inflammatory thresholds to irritants and haptens. J Allergy Clin Immunol 2009;124:496-506, e1-6.
18. Jarrett A, Spearman RI. The keratin defect and hair-cycle of a new mutant (matted) in the house-mouse. J Embryol Exp Morphol 1957;5:103-10.
19. Lane PW. Two new mutations in linkage group XVI of the house mouse. Flaky tail and varitint-waddler-J. J Hered 1972;63:135-40.
20. Searle A, Spearman R. "Matted," a new hair-mutant in the house-mouse: genetics and morphology. J Embryol Exp Morphol 1957;5:93-102.
21. Kezic S, Kemperman PM, Koster ES, de Jongh CM, Thio HB, Campbell LE, et al. Loss-of-function mutations in the filaggrin gene lead to reduced level of natural moisturizing factor in the stratum corneum. J Invest Dermatol 2008;128:2117-9.
22. O'Regan GM, Kemperman PM, Sandilands A, Chen H, Campbell LE, Kroboth K, et al. Raman profiles of the stratum corneum define 3 filaggrin genotype-determined atopic dermatitis endophenotypes. J Allergy Clin Immunol 2010;126:574-580.e1.
23. Proksch E, Folster-Holst R, Jensen JM. Skin barrier function, epidermal proliferation and differentiation in eczema. J Dermatol Sci 2006;43:159-69.
24. Fluhr JW, Elias PM, Man MQ, Hupe M, Selden C, Sundberg JP, et al. Is the filaggrin-histidine-urocanic acid pathway essential for stratum corneum acidification? J Invest Dermatol 2010;130:2141-4.
25. Brody I. The keratinization of epidermal cells of normal guinea pig skin as revealed by electron microscopy. J Ultrastruct Res 1959;2:482-511.
26. Brody I. The ultrastructure of the tonofibrils in the keratinization process of normal human epidermis. J Ultrastruct Res 1960;4:264-97.
27. Norlen L, Al-Amoudi A. Stratum corneum keratin structure, function, and formation: the cubic rod-packing and membrane templating model. J Invest Dermatol 2004;123:715-32.
28. Kawamoto T. Use of a new adhesive film for the preparation of multi-purpose fresh-frozen sections from hard tissues, whole-animals, insects and plants. Arch Histol Cytol 2003;66:123-43.
29. Kubo A, Nagao K, Yokouchi M, Sasaki H, Amagai M. External antigen uptake by Langerhans cells with reorganization of epidermal tight junction barriers. J Exp Med 2009;206:2937-46.
30. Ouchi T, Kubo A, Yokouchi M, Adachi T, Kobayashi T, Kitashima DY, et al. Langerhans cell antigen capture through tight junctions confers preemptive immunity in experimental staphylococcal scalded skin syndrome. J Exp Med 2011;208:2607-13.
31. Nagao K, Ginhoux F, Leitner WW, Motegi S, Bennett CL, Clausen BE, et al. Murine epidermal Langerhans cells and langerin-expressing dermal dendritic cells are unrelated and exhibit distinct functions. Proc Natl Acad Sci U S A 2009;106:3312-7.
32. Larson RP, Zimmerli SC, Comeau MR, Itano A, Omori M, Iseki M, et al. Dibutyl phthalate-induced thymic stromal lymphopoietin is required for Th2 contact hypersensitivity responses. J Immunol 2010;184:2974-84.
33. Nemoto-Hasebe I, Akiyama M, Nomura T, Sandilands A, McLean WH, Shimizu H. Clinical severity correlates with impaired barrier in filaggrin-related eczema. J Invest Dermatol 2009;129:682-9.
34. Manabe M, Sanchez M, Sun TT, Dale BA. Interaction of filaggrin with keratin filaments during advanced stages of normal human epidermal differentiation and in ichthyosis vulgaris. Differentiation 1991;48:43-50.
35. Sybert VP, Dale BA, Holbrook KA. Ichthyosis vulgaris: identification of a defect in synthesis of filaggrin correlated with an absence of keratohyaline granules. J Invest Dermatol 1985;84:191-4.
36. Gruber R, Elias PM, Crumrine D, Lin TK, Brandner JM, Hachem JP, et al. Filaggrin genotype in ichthyosis vulgaris predicts abnormalities in epidermal structure and function. Am J Pathol 2011;178:2252-63.

METHODS

Generation of *Flg*$^{-/-}$ mice

Flg$^{-/-}$ mice were generated by means of homologous recombination. The murine filaggrin gene *(Flg)*, which is located on chromosome 3, consists of 3 exons and shares unique characteristics with its human counterpart. Exon 1 consists of 5′ UTR sequences, exon 2 contains the translation start site, and the unusually large exon 3 encodes filaggrin repeats that are almost identical with each other, flanked by a 5′-specific sequence encoding the S-100 domain and a 3′-specific sequence followed by a 3′-UTR (Fig E1, *A*). Large open reading frames and repetitive sequences complicated the strategy by which the genes were targeted.

We designed the targeting vector to remove both the start codon located in exon 2 and in-frame ATG sequences located at the 5′-end of exon 3, which excluded all in-frame ATG sequences in *Flg*. The 3′ short homology arm was designed to include 5′-specific *Flg* sequences and part of the first filaggrin repeat (Fig E1, *A*) to minimize the possibility of unexpected recombination within the filaggrin repeats. Electroporation of the targeting vector into C57BL/6 ES cells did not yield any appropriately recombined ES cells. Using BA1 hybrid (C57BL/6 × 129/SvEv background) ES cells, we successfully obtained an ES cell clone named 824 in which homologous recombination between the targeting vector and *Flg* at the side of the long homology arm was confirmed by means of Southern blotting of *Bam*HI-digested genomic DNA by using a probe specific for the outside of the long homology arm (Fig E1, *A*, blue; wild-type = 11.8 kb; F1 hetero = 9.1 kb; data not shown). ES cell clone 824 was injected into C57BL/6 blastocysts, and chimeric mice were obtained. One of the chimeric mice was crossed with a C57BL/6 wild-type mouse. Southern blotting analysis of *Bam*HI-digested genomic DNA of F1 generation mice with the above probe successfully identified F1 hetero mice (Fig E1, *B*). To confirm successful recombination at the side of the short homology arm and integration of only 1 copy of the targeting vector, we performed Southern blotting with a probe specific for the 5′-specific *Flg* sequence located within the short homology arm. When genomic DNA from wild-type C57BL/6 and 129/SvEv mice was digested by *Msc*I and analyzed by means of Southern blotting with this probe (Fig E1, *A*, red), a 6-kb band and a 10-kb band were detected, respectively, indicating the existence of a polymorphism within the filaggrin repeats (Fig E1, *C*). Because the amount of genomic DNA excluded by means of gene targeting was almost the same as the size of the neomycin cassette of the targeting vector, successfully targeted mice were predicted to produce same-sized bands as wild-type mice (Fig E1, *A*). Although only a 6-kb band was detected in F1 hetero mice, both 6- and 10-kb bands were detected in their wild-type littermates, indicating that the C57BL/6 *Flg* allele had been targeted (Fig E1, *C*). These results also indicated the integration of a single copy of the targeting vector and the absence of unexpected homologous recombination between the short homology arm and filaggrin repeat sequences. Mice were backcrossed to C57BL/6 and BALB/c backgrounds to minimize phenotypic variation, especially in the context of immune response analyses.

Southern blotting

Genomic DNA from ES cells, mice tails, and hepatics was digested with the appropriate restriction enzymes. DNA fragments were separated by using 0.7% agarose gel electrophoresis, transferred to GeneScreen Plus membranes (NEN Life Science Products), and hybridized at 65°C with phosphorous 32–labeled insert cDNA.

Antibodies

Antibodies against filaggrin (Covance, Berkeley, Calif), involucrin, loricrin, keratin 1 (all Abcam, Cambridge, Mass), and actin (Santa Cruz Biotechnology, Santa Cruz, Calif) were used for immunoblotting and immunohistochemistry.

Immunoblotting

Urea/Tris extracts were prepared from 5-day-old mice, as described previously.[E1] Protein samples were fractionated by means of SDS-PAGE and transferred to Immobilon-P membranes (Millipore, Bedford, Mass). Membranes were treated with primary antibodies. Bound primary antibody was detected with an alkaline phosphatase–conjugated secondary antibody (Zymax, San Francisco, Calif).

Histologic analysis

Skin specimens were fixed in 10% buffered formalin and embedded in paraffin. For immunohistochemical analysis, primary antibodies were detected with an ImmPRESS Reagent kit (Vector Laboratories, Burlingame, Calif). For frozen sections, tissues were embedded in Tissue-Tek OCT compound (Sakura Finetechnical, Tokyo, Japan) in a liquid nitrogen–cooled isopentane bath. Safranin staining was performed to enhance visualization of SC layers, as described previously.[E2]

Negative replica imaging

Negative replica images of the dorsal skin surface in neonatal mice were obtained by using SILFLO (Flexico Developments Ltd, Potters Bar, United Kingdom), a silicon-based gum material, and were analyzed with laser profilometry (Primos; GFMesstechnik GmbH, Teltow, Germany).

Biophysical skin measurements

For the analysis of amino acid content, SC samples were obtained from 1.5 × 2.0–cm^2 regions of dorsal skin in 4-day-old neonatal mice through 6 rounds of TS (Scotch tape; 3M, St Paul, Minn). The SC was detached from the tape with toluene. After the solvent was evaporated, amino acids were extracted with 10% sulphosalicylic acid solution and subjected to amino acid analysis with an amino acid analyzer (Hitachi, Tokyo, Japan).

NMF, lipid, and water concentration profiles in murine SC were analyzed by using *in vivo* confocal Raman microspectroscopy (Model 3510 Skin Composition Analyzer; River Diagnostics, Rotterdam, The Netherlands) with previously described methods.[E3] Molecule concentration profiles in the abdominal SC of 2- to 5-day-old neonatal mice were measured at intervals of 2 μm to a depth of 8 μm. Raman spectra were recorded in the spectral region at 400 to 1800 cm^{-1} with a 785-nm laser for the measurement of NMF and lipid components and at 1500 to 3800 cm^{-1} with a 671-nm laser for the measurement of water. NMFs were measured as the sum of the spectra for the dominant constituents (serine, glycine, pyrrolidone-5-carboxylic acid, proline, ornithine, histidine, and alanine) by using the signal intensity of the Raman spectrum for keratin as the reference value. The water/protein ratio was calculated as the ratio between the Raman signal intensity of water (caused by OH-stretching vibrations) integrated from 3350 to 3550 cm^{-1} and that of protein (caused by CH_3-stretching vibrations) integrated from 2910 to 2965 cm^{-1} to determine SC water concentrations.

SC lipid contents of lipid extracts isolated from SC sheets from the same area were measured. Epidermal sheets were obtained from 10 mmol/L dithiothreitol-treated skin and were then incubated for 10 minutes at 37°C in 0.25% trypsin solution. After incubation, samples were gently vortexed to remove residual nucleated cells and washed with PBS 3 times. SC lipids were extracted from these SC sheets and analyzed by using high-performance thin-layer chromatography, as described previously.[E4]

Measurements of SC conductance, TEWL, and SC surface pH were performed at room temperature (22°C-26°C) and 40% to 60% humidity. SC hydration was evaluated by analyzing skin electrical impedance[E5] with a Corneometer ASA-M2 (Asahi Biomed, Yokohama, Japan).[E6] TEWL was measured with a VAPOSCAN AS-VT100RS machine (Asahi Biomed). SC surface pH was evaluated with the skin pH meter PH 905 (Courage & Khazaka, Cologne, Germany). All data are presented as the median of 3 repeated recordings.

Electron microscopy

For low-vacuum scanning electron microscopic analysis, feet, tails, and dorsal and abdominal skin were harvested from P5 neonatal mice and fixed in glutaraldehyde. After dehydration in tert-butyl alcohol, samples were observed with a low-vacuum scanning electron microscope (S-3400N; Hitach High-Tech, Tokyo, Japan).

Skin samples were fixed with 2% glutaraldehyde and 1% osmium tetroxide and processed for conventional TEM. For visualization of SC structures, skin

samples were fixed with half-strength Karnovsky fixative and then with 0.2% ruthenium tetroxide and 0.5% potassium ferrocyanide in 0.1 mol/L sodium cacodylate (pH 6.8).[E7]

Fragility assay

The dorsal skin of P4 neonatal mice was repeatedly tape stripped at the same sites with Cryofilm Type 2C (Leica Microsystems, Tokyo, Japan) to assess the detachment of cornified layers under mechanical stress. The amount of detached cornified material on the tape was evaluated by using a modified form of the DIA described previously.[E8] Briefly, light transmission images of cornified materials on the tape were acquired by using an Axio Observer Z1 microscope (Carl Zeiss, Oberkochen, Germany) equipped with a ×5 objective and were analyzed with Image Pro Plus version 6.2 software (Media Cybernetics, Inc, Silver Spring, Md). Within the observed area, the grayscale pixel distribution ranging from 0 (black) to 255 (white) was determined. The desquamation index was calculated as follows:

$$\text{Desquamation index} = \sum_{n=1}^{255} A_n \times n,$$

where *An* denotes the number of pixels at gray level *n*. Calculation of the desquamation index is based on the assumption that the whiteness of the scales is roughly proportional to their thickness.[E9]

Permeability assay

A saturated solution of calcein (Bis[N,Nbis(carboxymethyl)aminomethyl] fluorescein; Sigma-Aldrich) or calcein solution including calcein encapsulated in liposomes prepared from Presome CSII-101 (Nippon Fine Chemical, Osaka, Japan).[E10] was topically applied to the tails of 6- to 8-week-old mice for 3 hours. The tails were then removed and rapidly freeze embedded.

The Kawamoto film method was used, with modifications, for accurate evaluation because it prevents diffusion of fluorescence and preserves tissue components during sample preparation.[E11] Cryofilm was fastened to the cut surfaces of the samples to allow nondamaged SC to be visualized, and freeze sectioning was performed. Permeability was evaluated by using confocal microscopy without fixing to prevent the oozing of fluorescent substances.

Serum antibody analysis

OVA-specific antibody levels were measured by using ELISA. For the analysis of OVA-specific IgE levels, 96-well MaxiSorp ELISA plates (Nunc, Roskilde, Denmark) were coated with capture IgE antibody by using a murine IgE quantitative ELISA kit (Bethyl Laboratories, Montgomery, Tex) for 60 minutes and then blocked with 3% skim milk in PBS for 60 minutes. After blocking, serum samples (50 μL) diluted in Can Get Signal Solution 1 (TOYOBO, Tokyo, Japan) to an appropriate concentration were added to appropriate wells, and the plate was incubated for 60 minutes. After washing, OVA (1.5 μg/mL in Can Get Signal Solution 1) was added to each well, and the plate was incubated for 60 minutes. Horseradish peroxidase–conjugated anti-OVA (Rockland, Gilbertsville, Pa; diluted 1:10,000 in Can Get Signal Solution 2) was added for 60 minutes. TMB substrate was applied, and the absorbance at 450 nm was measured.

For the analysis of OVA-specific IgG_1 levels, plates were coated with OVA (10 μg/mL in PBS) at 4°C overnight. After blocking, 500-fold diluted sera were added to appropriate wells, and the plate was incubated for 2 hours. Horseradish peroxidase–conjugated anti-mouse IgG_1 (100 μL, dilution 1:10,000, Bethyl Laboratories) was applied for 2 hours to conjugate the antigen-antibody complex. TMB substrate was applied, and the absorbance at 450 nm was measured.

REFERENCES

E1. Presland RB, Boggess D, Lewis SP, Hull C, Fleckman P, Sundberg JP. Loss of normal profilaggrin and filaggrin in flaky tail (ft/ft) mice: an animal model for the filaggrin-deficient skin disease ichthyosis vulgaris. J Invest Dermatol 2000; 115:1072-81.

E2. Ya-Xian Z, Suetake T, Tagami H. Number of cell layers of the stratum corneum in normal skin—relationship to the anatomical location on the body, age, sex and physical parameters. Arch Dermatol Res 1999;291:555-9.

E3. Caspers PJ, Lucassen GW, Carter EA, Bruining HA, Puppels GJ. In vivo confocal Raman microspectroscopy of the skin: noninvasive determination of molecular concentration profiles. J Invest Dermatol 2001;116:434-42.

E4. Weerheim A, Ponec M. Determination of stratum corneum lipid profile by tape stripping in combination with high-performance thin-layer chromatography. Arch Dermatol Res 2001;293:191-9.

E5. Yamamoto Y. Measurement and analysis of skin electrical impedance. Acta Derm Venereol Suppl (Stockh) 1994;185:34-8.

E6. Tomita Y, Akiyama M, Shimizu H. Stratum corneum hydration and flexibility are useful parameters to indicate clinical severity of congenital ichthyosis. Exp Dermatol 2005;14:619-24.

E7. Hou SY, Mitra AK, White SH, Menon GK, Ghadially R, Elias PM. Membrane structures in normal and essential fatty acid-deficient stratum corneum: characterization by ruthenium tetroxide staining and x-ray diffraction. J Invest Dermatol 1991;96:215-23.

E8. Soma Y, Kashima M, Imaizumi A, Takahama H, Kawakami T, Mizoguchi M. Moisturizing effects of topical nicotinamide on atopic dry skin. Int J Dermatol 2005;44:197-202.

E9. El Gammal C, Pagnoni A, Kligman AM, el Gammal S. A model to assess the efficacy of moisturizers—the quantification of soap-induced xerosis by image analysis of adhesive-coated discs (D-Squames). Clin Exp Dermatol 1996;21: 338-43.

E10. El Maghraby GM, Barry BW, Williams AC. Liposomes and skin: from drug delivery to model membranes. Eur J Pharm Sci 2008;34:203-22.

E11. Kawamoto T. Use of a new adhesive film for the preparation of multi-purpose fresh-frozen sections from hard tissues, whole animals, insects and plants. Arch Histol Cytol 2003;66:123-43.

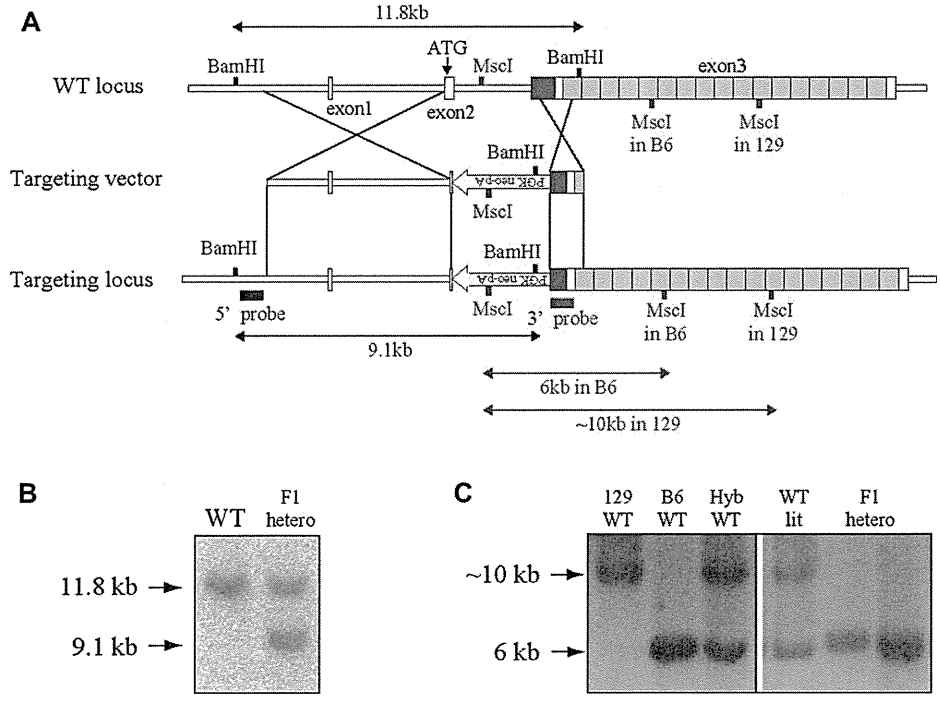

FIG E1. A, Partial restriction enzyme maps and schematic representation of the strategy used to ablate *Flg* expression in mice. **B** and **C,** Southern blot analyses with *Bam*HI-digested (Fig E1, *B*) and *Msc*I-digested (Fig E1, *C*) genomic DNA were performed to confirm the successful recombination at the sides of the long (Fig E1, *B*) and short (Fig E1, *C*) homology arms, respectively. *WT*, Wild-type.

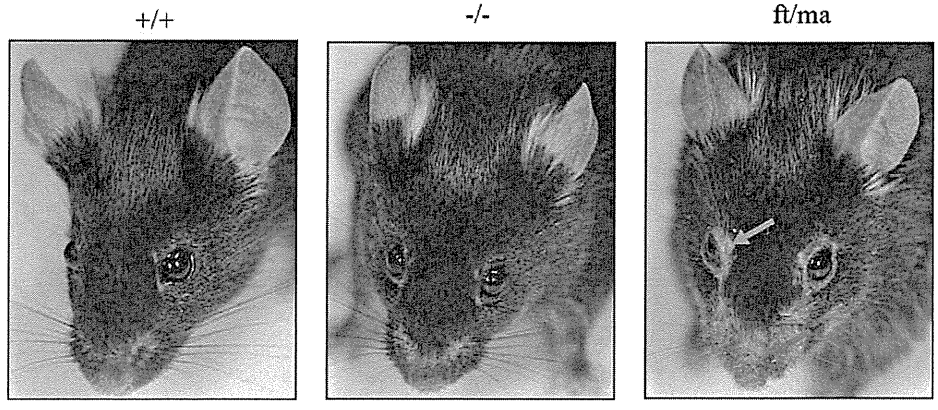

FIG E2. Clinical photographs of 12- to 15-week-old wild-type *(+/+)*, *Flg*$^{-/-}$ *(−/−)*, and ft/ma mice under SPF conditions. Whereas ft/ma mice had dermatitis *(arrows)* spontaneously, *Flg*$^{-/-}$ mice did not have any cutaneous manifestation.